GRASP55 is dispensable for normal hematopoiesis but necessary for Myc-dependent leukemic growth.

Anne-Laure Bailly, Julien Grenier, Amandine Cartier-Michaud, Florence Bardin, Marielle Balzano, Armelle Goubard, Jean-Claude Lissitzky, Maria de Grandis, Stéphane Mancini, Arnaud Sergé, et al.

GRASP55 is dispensable for normal hematopoiesis but necessary for Myc-dependent leukemic growth.

Anne-Laure Bailly[*], Julien M.P. Grenier[*], Amandine Cartier-Michaud[*], Florence Bardin[*], Marielle Balzano[*], Armelle Goubard[*], Jean-Claude Lissitzky[*], Maria De Grandis†, Stéphane J.C. Mancini[*], Arnauld Sergé[*] and Michel Aurrand-Lions[*#]

Running title: Grasp55 is dispensable for normal hematopoiesis

[*]Aix Marseille University, CNRS, INSERM, Institut Paoli-Calmettes, CRCM, Marseille, France. Equipe Labellisée Ligue Contre le Cancer.

†EFS PACA Corse, « Biologie des Groupes Sanguins », UMR 7268, Aix Marseille Université, CNRS

[#]Address correspondence to: MAL Cancerology Research Center of Marseille, CRCM, 27 Boulevard Leï Roure CS3005913273 Marseille Cedex 09 France

Tel:+33 (0)4 86 97 72 91 Fax:+33 (0)4 86 97 74 99

Mail: michel.aurrand-lions@inserm.fr

Grant support:

This work was partly supported by grants from the French National Research Agency (ANR #BSV1 019 02), Cancéropôle PACA, the ARC Foundation (PJA#20141201990 to MAL, PJA# 20131200298 to SJM and PJA#20131200238 to AS), the A*MIDEX project (#ANR-11-IDEX-0001-02) and the FEDER, funded by the "Investissements d'Avenir" French Government Program and managed by the French National Research Agency (ANR). ALB and MB were respective PhD student recipients of grants LNCC (TDQR15906) and FRM (#FDT20150532380). The funders had no role in study design, data collection and analysis, decision to publish, or preparation of the manuscript.

Abstract

Grasp55 is a ubiquitous Golgi stacking protein involved in autophagy, protein trafficking and glucose deprivation sensing. The function of Grasp55 in protein trafficking has been attributed to its PDZ-mediated interaction with the c-terminal "PDZ binding motifs" of protein cargos. We have recently shown that such an interaction occurs between Grasp55 and the adhesion molecule Jam-C which plays a central role in stemness maintenance of hematopoietic and spermatogenic cells. Accordingly, we have found that *Grasp55*-deficient mice suffer from spermatogenesis defects similar to *Jam-C* knock-out mice. However, whether Grasp55 is involved in the maintenance of immuno-hematopoietic homeostasis through regulation of protein transport and Jam-C expression remains unknown. Here, we show that *Grasp55* deficiency does not affect hematopoietic stem cell differentiation, engraftment or mobilization, which are known to depend on expression of Grasp55-dependent protein cargos. In contrast, using a Myc-dependent leukemic model addicted to autophagy, we show that knock-down of Grasp55 in leukemic cells reduces spleen and bone marrow tumor burden upon intravenous leukemic engraftment. This is not due to reduced homing of Grasp55-deficient cells to these organs but to increased spontaneous apoptosis of Grasp55-deficient leukemic cells correlated with increased sensitivity of the cells to glucose deprivation. These results show that Grasp55 plays a role in Myc-transformed hematopoietic cells but not in normal hematopoietic cells *in vivo*.

Key points:

- Golgi morphology and *Grasp55* expression are regulated during hematopoiesis
- Hematopoiesis is not affected in *Grasp55*-deficient mice
- Grasp55 regulates Myc-transformed leukemic cell survival

Introduction

Hematopoiesis and spermatogenesis are two differentiation processes in which adult stem cells produce their progeny in a sequentially ordered manner. It has been shown previously that JAM-C is expressed by hematopoietic stem cells (HSC) and by male germ cells (1-3). In both biological models, JAM-C plays a role in the maintenance of tissue homeostasis through adhesion regulation between developing cells and surrounding stromal cells expressing JAM-B, the high affinity ligand of JAM-C (4, 5). During spermatogenesis, JAM-C regulates polarization of developing spermatids, a critical step in spermatozoa development (3). During hematopoiesis, JAM-C interaction with JAM-B plays a critical role in maintenance of hematopoietic stem cells (HSC) which are at the apex of hematopoietic hierarchy (6). HSC differentiate into more mature multipotent progenitors (MPPs) which have decreased self-renewal capacity and progressively engage in megakaryocyte (MPP2), myeloid biased (MPP3) or lymphoid biased (MPP4) multipotent progenitors (7). In agreement with its function in HSC maintenance, JAM-C is downregulated in MPPs during steady state hematopoiesis (2). JAM-C expression by HSC is also rapidly downregulated after HSC mobilization using Cyclophosphamide and G-CSF (8), suggesting that JAM-C may play a role in the switch from steady state to emergency hematopoiesis. However, down-regulation of JAM-C is not unique to G-CSF-induced mobilization since down-regulation of other bone marrow retention signals such as VCAM-1/VLA-4, CXCL12/CXCR4 or SCF/Kit have also been documented (9-11).

We have recently identified the Golgi-reassembly stacking protein of 55kDa (Grasp55) as a PDZ-domain containing protein interacting with the C-terminal PDZ-binding motif of Jam-B and Jam-C in mouse (12). Grasp55, and the related protein Grasp65, are highly conserved throughout evolution and play complementary roles in Golgi cisternal stacking through oligomerization and PDZ-mediated interactions with proteins of the golgin family such as

Golgin45, GM130 or p24 (13-17). In addition, GRASP55 depletion results in accelerated protein trafficking through the Golgi apparatus and has striking negative effects on protein glycosylation and sorting (18). More recently, O-GlcNAcylation has been shown to restrict the function of GRASP55 to Golgi stacking, while de-O-GlcNAcylation switches its function as an autophagosome-lysosome tethering molecule (19). However, the function of GRASP55 is not limited to Golgi stacking and autophagy regulation since several studies have shown that GRASP55 is involved in protein trafficking through an unconventional secretory pathway triggered by cellular stress or unfolded protein response (UPR) (20-23). TGF-β, MT1-MMP, membrane bound SCF, CD8α, Frizzled4, CD83 and IL1β have been shown to be transported in a GRASP55-dependent manner (24-28). In addition, GRASP55 has been involved in MT1-MMP activation which is necessary for various biological processes, including HSC mobilization (29). We have thus explored the function of GRASP55 in adult mammalian normal and pathological hematopoiesis. To this end, we have generated constitutive and inducible knock-out mouse models of *Gorasp2* (encoding Grasp55) and studied HSC self-renewal, engraftment, mobilization and differentiation. To test whether Grasp55 may be involved in pathological hematopoiesis, we also questioned whether Grasp55 controls leukemic development. To this end, we used the Eμ-Myc lymphoma model known to be addicted to autophagy activation (30, 31).

Our results show that Grasp55 is not involved in the regulation of JAM-C expression in HSC. In addition, Grasp55-deficiency does not affect HSC maintenance or differentiation at steady state or upon hematopoietic stress. We further show that this is not due to compensatory mechanisms since acute depletion of Grasp55 expression using Mx1-Cre inducible system does not result in hematopoietic abnormalities. This is likely due to the inversely regulated expression of Grasp55 and Jam-C during hematopoietic cell differentiation. Indeed, Grasp55 transcript and protein are expressed at low levels in the most immature hematopoietic cells

(HSC-MPP1) and are upregulated in the following differentiation steps (MPP2 and MPP3-4) in which JAM-C expression is lost. We thus tested whether Myc-induced B cell lymphoid leukemia would depend on Grasp55 expression for their growth. Our results show that Grasp55 is necessary for Myc-dependent lymphoid leukemic development *in vivo*, opening the way for specific Grasp55 targeting in Myc-addicted hematological malignancies.

Material and Methods

Mice

Generation and genotyping of *Gorasp2* constitutive deficient mice were previously described (Cartier-Michaud et al.). Because *Gorasp2* deficient male are sterile, the colony is maintained by interbreeding of heterozygote mice. The colony was backcross on C57/BL6J mice more than 10 generation. Floxed *Gorasp2* lines, obtained before CMV-Cre deleter mice mating during Gorasp2 knockout generation, are maintained by intercrossing and backcrossing on C57/BL6 background more than 7 generation. Conditional inducible *Grasp55* (*Gorasp2)* deficient mice were obtained by two successive mating: in a first time $Grasp55^{-/-}$ female were mated with Mx1-cre^{Pos} male mice to obtained $Grasp55^{+/-}$ $Mx1\text{-}Cre^{Pos}$ mice, in a second time $Grasp55^{+/-}$ Mx1-Cre^{Pos} mice are mated with $Grasp55^{fl/fl}$ mice. $Grasp55^{fl/-}$ Mx1-Cre^{Neg} and $Grasp55^{fl/-}$ Mx1-Cre^{Pos} mice were used for experimentation. Same strategy was used to obtain hematopoietic-specific constitutive $Grasp55^{fl/-}$ Vav-Cre mice, $Gorasp2^{fl/-}$ Vav-Cre^{Neg} ($Grasp55^{WT}$ and $Gorasp2^{fl/-}$ Vav-Cre^{Pos} ($Grasp55^{\Delta Hem}$) mice were used for experimentation. CD45.1/2 mice used as competitor in competitive assay were obtained by interbreeding of CD45.1 with CD45.2 mice (purchased from JANVIER LABS). Mice were used at age more than 8 weeks old. All animal experiments were performed according to French Guidelines for Animal Handling in CRCM animal facility (Agreement D13 055 04). Experimental protocols were approved by the Ethical Committee #14 under the declaration number #02294.01.

Genotyping

Genotyping of *floxed Grasp55* line was achieved by PCR of genomic DNA extracted from mouse tails using the same primers and conditions as constitutive *Gorasp2* mice. But resulting in an amplification of 544-bp fragment for the WT allele and 700-bp fragment for the floxed allele were both obtained using heterozygous mice. Genotyping of Mx1-cre and Vav-cre mice

was achieved using the generic Cre and the iVav-Cre genotyping protocols from The Jackson Laboratory.

HSC exhaustion after 5-FU treatment

Grasp55^{WT} and *Grasp55*$^{\Delta Hem}$ mice were injected intraperitoneally once a week with 5-Fluoro-uracil (5-FU) at 120 mg/kg during 5 weeks. One day after 5-FU injection, blood paramaters were tested using IDEXX ProCyte Dx® Hematology Analyzer (IDEXX Laboratories). Mice were sacrificed at D35 after the first injection.

Inducible deletion with polyI:C and analysis of Grasp55 deletion

Gorasp2 gene deletion in *Gorasp2*$^{fl/-}$ *Mx1-Cre* mice was induced by three intraperitoneal injection of 200µg poly(I:C) (Invivogen) on day D0, D2 and D4. *Gorasp2* gene deletion in white blood cells (WBC) was confirmed on day 15 by PCR. Briefly, WBC isolated from 100µL of peripheral blood by Ficoll and genomic DNA was extracted by digestion in 250µl lysis buffer (50mM KCl, 10mM Tris pH 8,8, 2,5mM MgCl2, 0,45% NP40, 0,45% Tween) with 0.4mg/ml Proteinase K (Invitrogen) for 30min at 56°C, then PCR was achieved using same protocol as genotyping. Mice were sacrificed for analysis one month after the first poly(I:C) injection.

BM Mobilization Assays

Mobilization was induced using cyclophosphamide (CY, 4 mg i.p. d0) and rhG-CSF (5 mg s.c. at d1, 2, and 3) injections as previously described (8). Mice were sacrificed on day 5 for analysis.

Colony-Forming Assay

Peripheral blood and BM white blood cells were isolated by Ficoll. 200.000 blood cells were seeded per well in methylcellulose medium following the manufacturer's instructions (Stem Cell Technologies, Grenoble, France, www.stemcell.com, ref 3434).

Competitive Bone Marrow Transplantation

Lethally irradiated (8 grays) CD45.1 mice were transplanted with 2.10^6 of total bone marrow cell from donors (*Gorasp2*$^{+/+}$ or *Gorasp2*$^{-/-}$ CD45.2) and competitor (CD45.1/2) cells in a 1:1 ratio by retroorbital sinus injection. Mice chimerism was assessed monthly by monitoring of host (CD45.1), competitor (CD45.1/2) and donor (CD45.2) cells in peripheral blood by flow cytometry. Chimerism and hematopoietic phenotype in bone marrow were evaluated 18 weeks after transplantation.

Thioglycollate induced-peritonitis in chimeric mice

Lethally irradiated (8 grays) CD45.1 mice were transplanted with 2.10^6 of total bone marrow cell from donors (*Gorasp2*$^{+/+}$ or *Gorasp2*$^{-/-}$ CD45.2) by retro-orbital sinus injection. 18 weeks after transplantation, chimeric mice were injected intraperitoneally with 3ml of thioglycollate 3% (w/v; Sigma). 18 hours after injection, mice were sacrificed and peritoneal exudates were collected by three successive peritoneal washes with 10 ml cold phosphate buffer saline (PBS). Cells were counted and analyzed using IDEXX ProCyte Dx® Hematology Analyzer (IDEXX Laboratories).

EμMyc cells engraftment in mice

Mouse primary Eμ-Myc lymphoma cells were isolated as previously described (32) and expanded through passaging in irradiated recipient mice. 500.000 GRASP55^{KD} or Grasp55^{WT}

Eμ-Myc cells are injected into caudal tail vein of Ly5.1 mice. Mice were sacrificed at D9 after injection. Tumoral invasion in blood, spleen and bone marrow was assessed by flow cytometry.

Cytometry and cell sorting

Single cells suspensions were prepared from bone marrow (one leg: femur and tibia) and red blood cells were lysed with ACK (ammonium-chloride-potassium) buffer (Gibco). Cells were incubated with mAbs in PBS-0,5% BSA for 30 min at 4°C. For blood samples, RBC lysis was done after staining with BD FACS Lysing buffer (BD Bioscience). For hematopoietic cells identification, following antibodies were used: biotin anti-CD3, CD4, CD8, CD19, CD11c, DX5, Ter119, CD11b, B220, Gr1 (Lineage cocktail, Biolegend), CD16-32-PE (clone 2.4G2, BD Pharmingen), CD45.1-PECF594 (clone A20, BD Horizon), CD45.2-eF450 (clone104, eBioscience), CD48-PE-Cy7 (clone HM48-1, Biolegend), CD150-eF647 (clone TC15-12F12.2, Biolegend), CD117-APC-e780 (clone 2B8, eBioscience), CD127-PE-Cy5 (clone A7R34, eBioscience), CD135-PECF594 (clone A2F10.1, BD Horizon), Sca-1-BV421 (clone D7, BD Horizon) CD4-FITC (clone RAM4-5, eBioscience), CD8-PE (clone 53-6.7, eBioscience), B220-AF700 (clone RA3-6B2, eBiosciences), CD11b-APC (M1/70, eBioscience) and BV510-Streptavidin (BD Horizon). EμMyc cells were phenotyped using : CD19-BV500 (clone 1D3, BD Biosciences), CD23-BV711 (clone B3B4, BD Biosciences), CD25-PE-Cy5 (clone PC61, eBioscience), CD45.2-PE-Cy5.5 (clone 104, eBioscience), B220-APC-Cy7 (clone RA3-6B2, BD Biosciences), CD71-BV605 (clone C2, BD Biosciences), CD93-PE-Cy7 (clone AA4.1, eBioscience), BP1-biotin (clone BP1, BD Biosciences), streptavidin-AF594 (Biolegend). In all experiments a viability marker was used depending of the panels: SYTOX Green nucleic acid stain (Life Technologies), Fixable Viability Dye eF506 (eBioscience), DRAQ7 (Biostatus). JAM-B and JAM-C staining were

done using staining polyclonal rabbit anti-mouse JAM-B (pAb829) and JAM-C (pAb 501) produced in laboratory and R-Phycoerythrin conjugated goat-anti-rabbit IgG(H+L) antibody (1/200, Jackson Immunoresearch Laboratories) as secondary antibody. Grasp55 intracellular staining was done using anti-Grasp55 antibody (Protein-tech) and BD Cytofix/Cytoperm solution following the manufacture's instruction.

For hematopoietic stem and progenitor cells sorting, bone marrow cells were depleted using Lineage cell depletion Kit from Miltenyi and AutoMACS Pro. The Lin- cells were stained as described in preceding paragraph.

For Annexin-PI staining cells were stained with APC-AnnexinV (BD Bioscience) and propidium iodide solution (Sigma Aldrich) in Annexin binding buffer (Life Technologies) for 15 minutes at room temperature.

Stained cells were analyzed by a BD LSR-II FACS (lasers 405, 488, 561, and 633nm) and sorted by Aria III SORP sorter (BDBiosciences). Results were analyzed with BD-Diva version 8.0.1 software or FlowJo version 10.0.7 software (Treestar).

Cell culture

Eμ-Myc clone 504 cells were provided JE. Ricci. EμMyc cells were cultured in DMEM Glutamax, supplemented with 10% FBS, 1% non-essential amino acids, 1% L-glutamin, 1% Hepes 1mM, 1%PS, 0,1% β-mercaptoethanol (all cell culture products were purchased from Gibco). For cell proliferation, cells were plated at a density of 10.000 cells/well into 96-wells plate and cell numbers were quantified after 24, 48, 72, 96 hours using Cell Titer Glow Assay (Promega). *Grasp55*$^{+/+}$ and *Grasp55*$^{-/-}$ mouse embryonic fibroblasts (MEFs) were obtained as previously described (12). Chloroquine treatment was performed at a concentration of half IC50 (5μM for EμMyc cells and 17.5μM for MEFs) during 24 hours. For EμMyc glucose

starvation, cells were washed twice in PBS, incubated in DMEM without glucose (Gibco), 10% FCS, 1%PS and cells were quantified 24 hours later using Cell Titer Glow (Promega).

Lentiviral transduction

For lentiviral transduction, 1.10^6 cells were plated in 96-wells plates in 190µL complete medium with 8µg/ml polybrene and 10µl of lentiviral particles expressing Grasp55 shRNA-GFP ($GRASP55^{KD}$) or Control GFP ($GRASP55^{WT}$) vectors (TRIPdU3 vector). Cells were centrifuged at 3000 rpm without brake during 2h at 32°C and incubated overnight. Next day medium was replaced by complete medium and cell fluorescence was checked by microscopy (AMG EVOS LED fluorescence microscope). One week after transduction, transduced cells were sorted by flow cytometry based on GFP expression. Correct GRASP55 silencing was tested by Western blot.

Gene expression analysis

500 for each population (HSC-MPP1, MPP2, and MPP3-4) from WT CD45.1 mice were sorted using the autoclone module on an Aria III SORP sorter (BD Biosciences) into 96-well plates in the RT-STA Master Mix Solution. Cell lysis, cDNA synthesis, and amplification were performed according to Fluidigm protocols. Selected TaqMan Gene Expression assays (original magnification ×20) were pooled and diluted with water 100-fold so that each assay is at a final concentration of 0.2× in the pooled assay mix. Five microliters of CellsDirect 2× Reaction Mix (Invitrogen), 2.5 µl pooled assay mix, 0.2 µl SuperScript III RT/Platinum Taqmax mix, and 2.3 µl water were combined to a final volume of 10 µl in 1 well of a 96-well qPCR plate for the sort. cDNA samples were amplified using the following program (1): 50°C, 10 min (2); 95°C, 2 min (3); 95°C, 15 s (4); 60°C, 4 min; repeat steps (3) and (4) 18 times. Preamplified products were diluted 5-fold before analysis with Universal PCR Master

Mix and inventoried TaqMan gene expression assays in 96.96 Dynamic Arrays on a BioMark System (Fluidigm). For each gene, the relative expression was defined as the mean value of 40 minus cycle threshold for the gene of interest divided by 40 minus cycle threshold for actin. Results were represented as an heat map using Morpheus software (https://software.broadinstitute.org/*morpheus*/).

Western blot

GRASP-55 expression by hematopoietic cells was tested using a total of 10000-sorted cells for each population (HSC-MPP1, MPP2, MPP3-4) re-suspended in 50µl of RIPA buffer (50mM Tris HCl pH7.5, 150mM NaCl, 1% Triton, 0.1% SDS, 1% Na desoxylate) and 10µl of 6x sample buffer. Western blots for LC3 were performed on 20µg of proteins. Whole protein extracts were separated by SDS-PAGE and transfered onto nitrocellulose membrane. Saturated membranes were exposed to rabbit anti-GRASP55 antibody (1/500e ProteinTech), rabbit anti-LC3 antibody (1/1000e, MBL international corporation), mouse anti-α-tubulin antibody (1/1000, T6074 Sigma) in PBS-1% non-fat milk, 0,1% tween at 4°C overnight. Membranes were incubated with HRP-conjugated goat anti-rabbit IgG or HRP-conjugated goat anti-mouse IgG antibody (1/5000, Jackson Immunoresearch Laboratories) at RT one hour. Signal was revealed using SuperSignal West Pico Chemiluminescent substrate (ThermoFischer Scientific).

Immunofluorescence

1000 sorted cells were incubated in a 50µl PBS-0,5% BSA drop on poly L-lysine-coated slide in a humidified chamber at 37°C during 2 hours, buffer was carefully removed by aspiration and replaced by saturation mix (PBS-2%BSA).

Primary antibody anti-GRASP55 (ProteinTech, 1/250) was incubated overnight at 4°C in PBS-0,5% BSA. After soft washes, samples were incubated one hour at room temperature with donkey anti-rabbit-eF594-conjugated secondary probe purchased from Jackson Immunoresearch. DAPI nuclear staining was done with the second final wash. Coverslip was mounted using prolong gold antifade reagent (Invitrogen).

Images were obtained using a Zeiss LMS880 Meta confocal. Images were analyzed using Image J. Three dimensions Golgi volume quantification was performed as previously described (12).

Caspase activity assay

Cells were plated at a density of 10.000 cells/wells into a white walled 96-wells plate. Caspase activity was determined using the Caspase-Glo® 3/7 kit following the manufacturer's instructions (G811A from Promega®). Luminescence was measured using a POLARstar omega from BMG LABTECH.

In vivo homing

Eμ-myc GRASP55^{KD} were labeled with calcein violet (violet) and GFP (green) was used for Eμ-myc GRASP55^{WT} and injected at 1:1 ratio into mice (5.10^6 cells/200μL NaCl per mice). Cells in each organ were analyzed for expression of green or violet fluorescence by flow cytometry. Stained cells were analyzed by an LSRII FACS (lasers 405, 488, 561, and 633nm BDBiosciences). Results were analyzed with BD-Diva version 8.0.1 software.

Statistical Analysis

All experiments were performed at least 3 times. Statistical significance was performed using non-parametric Mann-Whitney U-test, Student t-Test or Two way ANOVA with Bonferroni post-test in Prism software. P-value less than 0.05 was considered as statistically significant.

Results

Regulated expression of GRASP55 during HSC differentiation

We first tested if *Gorasp2*, the gene encoding Grasp55, was expressed in hematopoietic stem and progenitor cells (HSPCs) using RT-qPCR on sorted cells from mouse bone marrow according to the gating strategy shown in Figure 1A. Although *Jam3*, the gene encoding Jam-C, was highly expressed on the most immature compartment (HSC-MPP1) and downregulated in more mature cells, *Gorasp2* presented an inverted pattern of expression and was barely detectable in HSC-MPP1 and MPP2 cells (Fig. 1B). Other genes encoding proteins involved in Golgi stacking such as *Blzf1* (encoding Golgin45) or *Golgb1* (encoding Giantin) followed the same pattern of expression as compared to *Gorasp2*, while expression of *Golga2* (encoding GM130) remained stable. Of note, and consistent with publicly available datasets from Immgen consortium (immgen.org), we failed to detect Gorasp1, the gene encoding Grasp65 in HSPC (not shown). Grasp55 upregulation between the most immature compartment (HSC-MPP1) and more differentiated multipotent progenitors (MPP2 and MPP3-4) was further confirmed at the protein level by flow cytometry and western-blotting (Fig. 1C-D). Immunostaining for Grasp55 performed on HSC-MPP1, MPP2 and MPP3-4 isolated from wild type or *Grasp55*$^{-/-}$ mice confirmed that Grasp55 expression and localization changed during hematopoietic cell differentiation (Fig. 1E). We found that Grasp55 signal was barely detectable in wild type HSC-MPP1 and was increased in MPP2 and MPP3-4, as confirmed by staining intensity quantification of confocal Z-stacked pictures (Fig. 1F). In addition, three dimensional quantification of Grasp55 staining revealed that the volume of Grasp55 vesiculo-tubular objects was not significantly different between HSC-MPP1 and MPP2 cells, while there was a significant increase in MPP3-4 cells (Fig. 1G). This indicates that Grasp55 is upregulated and recruited to large Golgi stacks at the transition

between MPP2 and MPP3-4 stages of differentiation, suggesting that structural Golgi remodeling occurs during hematopoietic differentiation.

Lack of hematopoietic and inflammatory defects in *Grasp55*$^{-/-}$ mice

We thus analyzed early hematopoietic differentiation in *Grasp55*$^{-/-}$ mice and compared to control littermate animals. Total number of bone marrow cells and percentages of Lin^{Neg}Sca^{Pos}Kit^{Pos} (LSK) were identical between *Grasp55*$^{+/+}$ and *Grasp55*$^{-/-}$ (Fig. 2A-B). Results were thus expressed as percentage of the LSK compartment (Fig. 2C) or percentage of total bone marrow (Fig. 2D). Within the LSK compartment, HSC-MPP1, MPP2 or MPP3-4 were not affected by the loss of Grasp55 expression (Fig. 2C), nor the more mature common myeloid progenitors (CMPs) or granulocyte/monocyte progenitors (GMP) (Fig. 2D). In addition, downregulation of JAM-C expression during hematopoietic differentiation was not affected suggesting that LT-HSC maintenance remained unaffected in absence of Grasp55 expression at steady state (Fig. 2E). We thus tested if Grasp55 may be involved in emergency hematopoiesis using constitutive hematopoietic specific Grasp55 deficient mice (Grasp55Δ^{Hem}) obtained by crossing *Grasp55*$^{fl/-}$ mice with Vav-Cre transgenic mice. Repeated injection of 5-Fluoro-Uracil (5-FU) resulted in similar decrease in hematocrit values between *Grasp55*^{WT} and Grasp55Δ^{Hem} animals (Supplementary Fig. 1A-B). The day 35 was defined as the endpoint for analysis of bone marrow composition to avoid death of the animals because of sustained anemia. No difference in absolute cell numbers or frequencies of early hematopoietic subsets was found between *Grasp55*$^{\Delta Hem}$ and *Grasp55*^{wt} control animals after 4 injections of 5-FU (Supplementary Fig. 1C-F). Although only three mice were analyzed in this pilot experiment, power calculation shows that a tremendous number of mice would have been necessary to get a chance to reach statistical significance. We thus decided to move to another model in which deletion of Grasp55 is induced in an acute manner to not

allow for compensatory mechanism to take place. To this end, Grasp55$^{fl/-}$ animals crossed with Mx1-cre transgenic mice were injected with poly(I:C) resulting in floxed allele deletion fifteen days upon poly(I:C) treatment (Supplementary Fig. 2A). Analysis of absolute bone marrow cell numbers and frequencies of LSK cells showed no differences between controls and conditional induced knock-out mice poly(I:C)-treated Grasp55$^{fl/-}$ Mx1-Cre mice (Supplementary Fig. 2B-C); nor did the analysis of different LSK (HSC-MPP1, MPP2, MPP3-4) and progenitor subsets (CMP, GMP) reveals difference between experimental groups (Supplementary Fig. 2D-E). Finally, since Grasp55 has also been involved in inflammatory response *in vitro* (23), we also tested whether inflammatory recruitment of leukocytes at effector sites would be affected by Grasp55 deficiency. Here again, we did not find significant differences in acute inflammatory recruitment of leukocytes to the peritoneal cavity upon thioglycollate challenge (Supplementary Fig. 3). This indicates that Grasp55 is dispensable for emergency hematopoiesis and inflammatory recruitment *in vivo*.

HSC mobilization and engraftment are not affected by *Grasp55* deficiency

Because Grasp55 has been involved in the regulation of retention signals for HSC in the bone marrow, we next performed HSC mobilization assays using Cyclophosphamide and G-CSF. This experimental setting induces dramatic changes in molecular mechanisms involved in HSC retention within BM niches and results in myeloid biased expansion of HSPCs (33). As expected, increase of LSK cells frequencies was found in mouse bone marrow and blood upon mobilization (Fig. 3A-B). However, such increase was independent of GRASP55 expression. When Colony Forming Unit-Cells (CFU-C) assays were performed as a read-out of hematopoietic cell progenitor activity, no differences were found between *Grasp55*$^{-/-}$ mice and control littermate animals (Fig. 3C). To get further insights into the function of GRASP55 in controlling cellular crosstalks upon hematopoietic stress, we performed competitive bone

marrow engraftment assays. To avoid bias due to the difference in CD45.1; CD45.2 and CD45.1/2 allele expression (34), we designed two experimental groups using CD45.2 *Grasp55*$^{+/+}$ or CD45.2 *Grasp55*$^{-/-}$ BM cells admixed at 1:1 ratios with wild-type CD45.1/2 bone marrow cells as competitors (Supplementary Fig. 4A). Engraftment was performed in CD45.1 lethally irradiated recipients (Fig. 4A). Such experiments are highly sensitive and have been widely used to highlight subtle defects in hematopoiesis which are not revealed in other experimental settings. Using chimerism measurement in the peripheral blood as follow-up, we found significant decrease in *Grasp55*$^{-/-}$ hematopoietic engraftment as compared to *Grasp55*$^{+/+}$ cells before 12 weeks, while differences disappeared at 16 weeks (Fig. 4B). This was mostly due to a reduction of *Grasp55*-deficient lymphoid cells in the blood circulation during the first four months after engraftment (Fig 4C-F). Such difference was abolished after 18 weeks, suggesting that this transient difference revealed subtle changes in the early steps of *Grasp55*-deficient cells commitment toward lymphoid versus myeloid lineage after engraftment. This is consistent with the high expression of Grasp55 found in MPP3-MPP4s myeloid and lymphoid biased progenitors (Fig.1). When chimerism in the bone marrow was analyzed after 18 weeks, overt engraftment advantage for wild-type competitor cells (CD45.1/2) against donor cells (CD45.2) was found in the LSK compartment irrespective of *Grasp55* genotype (Fig. 4G). No change in bone marrow cellularity was observed (Supplementary Fig. 4B). More interestingly, specific significant decrease in CMP frequencies was observed in mixed chimeric mice engrafted with *Grasp55*$^{-/-}$ and wild-type competitor cells as compared to *Grasp55*$^{+/+}$/wild-type chimeras while no change in GMP frequencies was detected (Fig. 4H). This was due to a significant decrease in competitor cell frequencies suggesting that loss of Grasp55 expression in hematopoietic cells may alter indirectly the maintenance of wild-type CMP.

GRASP55 plays a role in Myc-addicted leukemic growth *in vivo*

Since we failed to detect Grasp55-dependent alterations of the hematopoietic system at steady state or upon stress, we asked the question whether GRASP55 may contribute to development of Myc-addicted lymphoma/leukemia known to depend on autophagy pathway activation (30, 31, 35). One leukemic primary cell clone obtained from Eμ-Myc mice harbored a pre-B cell phenotype as demonstrated by positivity for CD19, CD25, CD43, BP1, CD93 (Fig. 5A). In addition, the selected clone expressed JAM-B, a known interacting partner of GRASP55 (Fig. 5B & (12)). Two cell lines in which GRASP55 expression was depleted or not were derived upon lentiviral transfection with shRNA directed against GRASP55 or empty vector containing the GFP only (Fig. 5C). Silencing GRASP55 did not affect JAM-B expression (not shown) nor cell proliferation (Fig. 5D). Upon engraftment in C57BL/6 animals, control Eμ-Myc cells invaded spleen and bone marrow within nine days, while invasion by Eμ-Myc GRASP55 knock-down cells (Eμ-Myc GRASP55^{KD}) was greatly reduced (Fig. 5E-F). This was accompanied by a three-fold decrease in peripheral leukemic cell load for Eμ-Myc GRASP55^{KD} leukemic cells as compared to control (Fig. 5G). Since such differences may rely on changes in homing or engraftment properties, we tested the tissue homing properties of the two cell lines. To this end, tissue homing was analyzed upon intra-vascular injection of mixed Eμ-Myc GRASP55^{WT} and Eμ-Myc GRASP55^{KD} cells, respectively labeled by GFP and GFP/Calcein violet reporters (Fig. 6A, left panel). Frequencies of Eμ-Myc GRASP55^{WT} cells were significantly increased as compared to Eμ-Myc GRASP55^{KD} cells in spleen, bone marrow and blood sixteen hours after injection (Fig 6B). This last result was surprising since reduced short term tissue homing is usually accompanied by increased number of cells remaining in the blood (36).

GRASP55 regulates cell survival in an autophagy independent manner

We thus hypothesized that Eμ-Myc GRASP55^{KD} cells may present reduced survival during early steps of homing experiments. Spontaneous apoptosis of Eμ-Myc GRASP55^{KD} cells was thus compared to Eμ-Myc GRASP55^{WT} cells. To this end, caspase activity was measured twelve hours after viable cell replating in fresh medium. A significant increase of caspase 3/7 activity was observed in Eμ-Myc GRASP55^{KD} cell culture as compared to control (Fig. 7A). Accordingly, we observed an increase in early and late apoptotic cells in Eμ-Myc GRASP55^{KD} cell culture as compared to Eμ-Myc GRASP55^{WT} (Fig. 7B-C). However, the effect was only marginal and would not totally explain results from *in vivo* homing experiments. Since normal value of glucose level in mouse serum is by far lower than in culture medium (1,4g/l versus 4g/l) and because GRASP55 has been involved in glucose sensing (37), we then reasoned that glucose starvation may be needed to reveal a more pronounced difference. We thus cultured Eμ-Myc leukemic cells for 96 hours in complete medium or in absence of glucose. Although more than 67% of Eμ-Myc GRASP55^{WT} cells survived glucose starvation, less than 55% of Eμ-Myc GRASP55^{KD} cells were still alive as compared to control culture condition in complete medium (Fig 7D). This result is consistent with a recent study showing that GRASP55 sense glucose deprivation to promote autophagosome-lysosome fusion (19). We then questioned whether such a pathway contributes to the better survival of Eμ-Myc proficient cells. To this end, we treated cells with chloroquine which is known to induce Eμ-Myc cell death through inhibition of lysosome function and autophagosome accumulation (38). We found no differences in cytotoxicity with respect to Grasp55 expression in Eμ-Myc cells or in mouse embryonic fibroblasts (MEFs) isolated from *Grasp55*$^{+/+}$ or *Grasp55*$^{-/-}$ mice (Fig. 8A). We confirmed that Myc transformed

460 cells were more sensitive to chloroquine than MEFs as previously reported (Fig. 8B & (38)).
461 However, we found no difference in LC3-II accumulation between Grasp55 proficient and
462 deficient cells at the steady state or upon chloroquine treatment (Fig. 8C-D). Altogether, these
463 results argue for an increased sensitivity to glucose starvation of Eμ-Myc Grasp55-deficient
464 cells without dramatic changes in autophagic fluxes.
465

Discussion

In the present study, we have addressed the physiological function of Grasp55 in normal, emergency and pathological hematopoiesis using *Grasp55*-deficient mice for which we have previously reported spermatogenesis defects (12). Surprisingly, we found no difference in normal and emergency hematopoiesis between Grasp55-deficient and proficient mice, even though Grasp55 has been involved in the regulation of number of molecules known to be essential for hematopoietic homeostasis. We rule out that this was due to incomplete deletion of the gene since mice presented overt phenotypes reminiscent of *Jam-c*$^{-/-}$ mice such as male infertility (3, 12, 39) which has been confirmed in another *Grasp55*-deficient strain (23). Although the absence of JAM-C deregulation in *Grasp55*$^{-/-}$ hematopoietic cells may be easily explained by the inverted expression pattern of JAM-C and GRASP55 during early hematopoietic cell differentiation (Fig. 1), the lack of overt immuno-hematopoietic phenotype remains puzzling. Indeed, given the roles of GRASP55 in Golgi structure, protein expression and autophagy (19, 23, 40, 41), one could expect dramatic effects due to the loss of GRASP55 expression when the hematopoietic system is challenged.

Several key regulators of hematopoietic homeostasis such as TGF-β, membrane bound SCF, or MT1-MMP have been shown to interact with GRASP55 (25, 29). TGF-β and membrane bound SCF interact with GRASP55 through canonical c-terminal PDZ binding motifs (25). Interaction of GRASP55 with transmembrane TGF-β was directly correlated to cell surface levels since mutation of the last two hydrophobic amino-acid (aa) reduced surface expression and GRASP55 interaction, while truncation of the last eight aa abolished interaction and expression. However, the reverse experiment consisting in silencing expression of GRASP55 and measuring TGF-β or membrane bound SCF expression were not performed in these studies. Thus, we cannot exclude that bone marrow stromal cells use alternative trafficking

491 machinery to express these niche factors. Our results are more difficult to reconcile with the
492 described function of GRASP55 in regulating MT1-MMP activation or IL1β secretion (23,
493 27, 29). Indeed, MT1-MMP activation by furin has been shown to depend on GRASP55 using
494 dominant negative approaches and overexpression of GRASP55 in HT1080 human
495 fibrosarcoma cell line (29). MT1-MMP plays a central role in maintenance of hematopoietic
496 homeostasis through the control of HIF1α and MMP2 activation (42, 43). The latter has been
497 shown to activate MMP9 which releases membrane-bound SCF upon HSC mobilization with
498 G-CSF (9). We failed to detect hematopoietic alterations at steady state homeostasis or upon
499 G-CSF-induced HSC mobilization in *Grasp55*$^{-/-}$ mice indicating that alternative pathways
500 regulating MT1-MMP activation must exist in bone marrow stromal cells. Same is true for
501 IL1β secretion. Indeed a first study has shown that silencing *Grasp55* expression in bone
502 marrow derived macrophages (BMDM) reduces IL1β secretion induced by nigericin and
503 starvation (27). A more recent study has demonstrated that IL1β secretion is reduced in
504 BMDM isolated from Grasp55-deficient mice due to impaired unfolded protein response
505 signaling (23). However, we found no differences in hematopoietic response upon 5-FU
506 treatment which is known to involve IL1β secretion by myeloid cells (44). This discrepancy
507 may be due to differences in the pathways involved in IL1β secretion by BMDM as compared
508 to IL1β secretion by the whole organism in response to hematopoietic stress. This raises the
509 question as to whether silencing Grasp55 in isolated cellular models reflects its physiological
510 function. Alternatively, it may well be that redundant unconventional secretory pathways are
511 present in higher eukaryotes and that compensatory mechanisms take place in absence of
512 Grasp55. Indeed, a single GRASP isoform is present in *Saccharomyces cerevisiae* and has
513 been involved in autophagic mediated secretion of Acb1 which lacks a signal sequence
514 similar to IL1β (45). This Grasp homologue represents the unique PDZ-containing protein of
515 yeast. This is in sharp contrast with the situation in mammals in which more than 250 PDZ

domains are present in more than 150 proteins (46). Therefore, it would be interesting to perform a shRNA screening against genes encoding PDZ containing proteins that could compensate *Gorasp2* deficiency for maintenance of hematopoietic stem cell homeostasis.

More interestingly, our results demonstrate that Eμ-Myc transformed hematopoietic cells become addict to Grasp55 pathway. Myc-dependent transformation is well known to induce unfolded protein response (UPR) which results in endoplasmic reticulum stress-induced autophagy (31). Autophagy promotes survival of tumor cells through processing cellular contents destined for degradation in order to support bioenergetics (30). Since Grasp55 has been involved in autophagy-driven pathways of unconventional secretion and in autophagosome-lysosome fusion upon glucose deprivation (19, 27, 45, 47), it may well be that the Eμ-Myc Grasp55^{KD} cells lose their ability to use autophagy as rescue mechanism and become sensitized to apoptosis. This would be consistent with previous findings showing that caloric restriction sensitizes Eμ-Myc cells to inhibitors of the antiapoptotic Bcl-2 protein family (48). It would therefore be interesting to explore effects of combined drug inhibition of Grasp55 and antiapoptotic proteins in additional cancer models known to involve UPR response and autophagy.

Acknowledgements

We are grateful to the flow cytometry, microscopy and animal core facilities for providing supportive help. We thank C. Bagnis and JE. Ricci who provided lentiviral stocks and primary lymphoma cells from Eμ-Myc mice, respectively.

Author contributions

ALB and JMPG designed and performed experiments, analyzed results, and wrote the manuscript. ACM, FB, MDG, MB and AG performed experiments. JCL performed lentiviral transductions. SJCM designed the flow cytometry panels and wrote the manuscript. AS performed imaging analysis. MAL supervised the study, analyzed results, discussed data and wrote the manuscript. All authors provided valuable inputs on the manuscript.

Additional information

The authors declare no competing interests.

References

1. Forsberg, E. C., S. S. Prohaska, S. Katzman, G. C. Heffner, J. M. Stuart, and I. L. Weissman. 2005. Differential expression of novel potential regulators in hematopoietic stem cells. *PLoS Genet* 1: e28.
2. Praetor, A., J. M. McBride, H. Chiu, L. Rangell, L. Cabote, W. P. Lee, J. Cupp, D. M. Danilenko, and S. Fong. 2009. Genetic deletion of JAM-C reveals a role in myeloid progenitor generation. *Blood* 113: 1919-1928.
3. Gliki, G., K. Ebnet, M. Aurrand-Lions, B. A. Imhof, and R. H. Adams. 2004. Spermatid differentiation requires the assembly of a cell polarity complex downstream of junctional adhesion molecule-C. *Nature* 431: 320-324.
4. Arrate, M. P., J. M. Rodriguez, T. M. Tran, T. A. Brock, and S. A. Cunningham. 2001. Cloning of human junctional adhesion molecule 3 (JAM3) and its identification as the JAM2 counter-receptor. *J Biol Chem* 276: 45826-45832.
5. Lamagna, C., P. Meda, G. Mandicourt, J. Brown, R. J. Gilbert, E. Y. Jones, F. Kiefer, P. Ruga, B. A. Imhof, and M. Aurrand-Lions. 2005. Dual interaction of JAM-C with JAM-B and alpha(M)beta2 integrin: function in junctional complexes and leukocyte adhesion. *Mol Biol Cell* 16: 4992-5003.
6. Arcangeli, M. L., V. Frontera, F. Bardin, E. Obrados, S. Adams, C. Chabannon, C. Schiff, S. J. Mancini, R. H. Adams, and M. Aurrand-Lions. 2011. JAM-B regulates maintenance of hematopoietic stem cells in the bone marrow. *Blood* 118: 4609-4619.
7. Pietras, E. M., D. Reynaud, Y. A. Kang, D. Carlin, F. J. Calero-Nieto, A. D. Leavitt, J. M. Stuart, B. Gottgens, and E. Passegue. 2015. Functionally Distinct Subsets of Lineage-Biased Multipotent Progenitors Control Blood Production in Normal and Regenerative Conditions. *Cell Stem Cell* 17: 35-46.
8. Arcangeli, M. L., F. Bardin, V. Frontera, G. Bidaut, E. Obrados, R. H. Adams, C. Chabannon, and M. Aurrand-Lions. 2014. Function of Jam-B/Jam-C interaction in homing and mobilization of human and mouse hematopoietic stem and progenitor cells. *Stem Cells* 32: 1043-1054.
9. Heissig, B., K. Hattori, S. Dias, M. Friedrich, B. Ferris, N. R. Hackett, R. G. Crystal, P. Besmer, D. Lyden, M. A. Moore, Z. Werb, and S. Rafii. 2002. Recruitment of stem and progenitor cells from the bone marrow niche requires MMP-9 mediated release of kit-ligand. *Cell* 109: 625-637.
10. Levesque, J. P., J. Hendy, Y. Takamatsu, P. J. Simmons, and L. J. Bendall. 2003. Disruption of the CXCR4/CXCL12 chemotactic interaction during hematopoietic stem cell mobilization induced by GCSF or cyclophosphamide. *J Clin Invest* 111: 187-196.
11. Levesque, J. P., Y. Takamatsu, S. K. Nilsson, D. N. Haylock, and P. J. Simmons. 2001. Vascular cell adhesion molecule-1 (CD106) is cleaved by neutrophil proteases in the bone marrow following hematopoietic progenitor cell mobilization by granulocyte colony-stimulating factor. *Blood* 98: 1289-1297.
12. Cartier-Michaud, A., A. L. Bailly, S. Betzi, X. Shi, J. C. Lissitzky, A. Zarubica, A. Serge, P. Roche, A. Lugari, V. Hamon, F. Bardin, C. Derviaux, F. Lembo, S. Audebert, S. Marchetto, B. Durand, J. P. Borg, N. Shi, X. Morelli, and M. Aurrand-Lions. 2017. Genetic, structural, and chemical insights into the dual function of GRASP55 in germ cell Golgi remodeling and JAM-C polarized localization during spermatogenesis. *PLoS Genet* 13: e1006803.

13. Barr, F. A., C. Preisinger, R. Kopajtich, and R. Korner. 2001. Golgi matrix proteins interact with p24 cargo receptors and aid their efficient retention in the Golgi apparatus. *J Cell Biol* 155: 885-891.
14. Xiang, Y., and Y. Wang. 2010. GRASP55 and GRASP65 play complementary and essential roles in Golgi cisternal stacking. *J Cell Biol* 188: 237-251.
15. Barr, F. A., N. Nakamura, and G. Warren. 1998. Mapping the interaction between GRASP65 and GM130, components of a protein complex involved in the stacking of Golgi cisternae. *EMBO J* 17: 3258-3268.
16. Zhao, J., B. Li, X. Huang, X. Morelli, and N. Shi. 2017. Structural Basis for the Interaction between Golgi Reassembly-stacking Protein GRASP55 and Golgin45. *J Biol Chem* 292: 2956-2965.
17. Bekier, M. E., 2nd, L. Wang, J. Li, H. Huang, D. Tang, X. Zhang, and Y. Wang. 2017. Knockout of the Golgi stacking proteins GRASP55 and GRASP65 impairs Golgi structure and function. *Mol Biol Cell* 28: 2833-2842.
18. Xiang, Y., X. Zhang, D. B. Nix, T. Katoh, K. Aoki, M. Tiemeyer, and Y. Wang. 2013. Regulation of protein glycosylation and sorting by the Golgi matrix proteins GRASP55/65. *Nat Commun* 4: 1659.
19. Zhang, X., L. Wang, B. Lak, J. Li, E. Jokitalo, and Y. Wang. 2018. GRASP55 Senses Glucose Deprivation through O-GlcNAcylation to Promote Autophagosome-Lysosome Fusion. *Dev Cell* 45: 245-261 e246.
20. Nickel, W., and C. Rabouille. 2009. Mechanisms of regulated unconventional protein secretion. *Nat Rev Mol Cell Biol* 10: 148-155.
21. Giuliani, F., A. Grieve, and C. Rabouille. 2011. Unconventional secretion: a stress on GRASP. *Curr Opin Cell Biol* 23: 498-504.
22. Gee, H. Y., S. H. Noh, B. L. Tang, K. H. Kim, and M. G. Lee. 2011. Rescue of DeltaF508-CFTR trafficking via a GRASP-dependent unconventional secretion pathway. *Cell* 146: 746-760.
23. Chiritoiu, M., N. Brouwers, G. Turacchio, M. Pirozzi, and V. Malhotra. 2019. GRASP55 and UPR Control Interleukin-1beta Aggregation and Secretion. *Dev Cell* 49: 145-155 e144.
24. D'Angelo, G., L. Prencipe, L. Iodice, G. Beznoussenko, M. Savarese, P. Marra, G. Di Tullio, G. Martire, M. A. De Matteis, and S. Bonatti. 2009. GRASP65 and GRASP55 sequentially promote the transport of C-terminal valine-bearing cargos to and through the Golgi complex. *J Biol Chem* 284: 34849-34860.
25. Kuo, A., C. Zhong, W. S. Lane, and R. Derynck. 2000. Transmembrane transforming growth factor-alpha tethers to the PDZ domain-containing, Golgi membrane-associated protein p59/GRASP55. *EMBO J* 19: 6427-6439.
26. Stein, M. F., K. Blume, C. S. Heilingloh, M. Kummer, B. Biesinger, H. Sticht, and A. Steinkasserer. 2015. CD83 and GRASP55 interact in human dendritic cells. *Biochem Biophys Res Commun* 459: 42-48.
27. Dupont, N., S. Jiang, M. Pilli, W. Ornatowski, D. Bhattacharya, and V. Deretic. 2011. Autophagy-based unconventional secretory pathway for extracellular delivery of IL-1beta. *EMBO J* 30: 4701-4711.
28. Nickel, W., and M. Seedorf. 2008. Unconventional mechanisms of protein transport to the cell surface of eukaryotic cells. *Annu Rev Cell Dev Biol* 24: 287-308.
29. Roghi, C., L. Jones, M. Gratian, W. R. English, and G. Murphy. 2010. Golgi reassembly stacking protein 55 interacts with membrane-type (MT) 1-matrix metalloprotease

(MMP) and furin and plays a role in the activation of the MT1-MMP zymogen. *FEBS J* 277: 3158-3175.

30. Amaravadi, R. K., D. Yu, J. J. Lum, T. Bui, M. A. Christophorou, G. I. Evan, A. Thomas-Tikhonenko, and C. B. Thompson. 2007. Autophagy inhibition enhances therapy-induced apoptosis in a Myc-induced model of lymphoma. *J Clin Invest* 117: 326-336.
31. Hart, L. S., J. T. Cunningham, T. Datta, S. Dey, F. Tameire, S. L. Lehman, B. Qiu, H. Zhang, G. Cerniglia, M. Bi, Y. Li, Y. Gao, H. Liu, C. Li, A. Maity, A. Thomas-Tikhonenko, A. E. Perl, A. Koong, S. Y. Fuchs, J. A. Diehl, I. G. Mills, D. Ruggero, and C. Koumenis. 2012. ER stress-mediated autophagy promotes Myc-dependent transformation and tumor growth. *J Clin Invest* 122: 4621-4634.
32. Chiche, J., S. Pommier, M. Beneteau, L. Mondragon, O. Meynet, B. Zunino, A. Mouchotte, E. Verhoeyen, M. Guyot, G. Pages, N. Mounier, V. Imbert, P. Colosetti, D. Goncalves, S. Marchetti, J. Briere, M. Carles, C. Thieblemont, and J. E. Ricci. 2015. GAPDH enhances the aggressiveness and the vascularization of non-Hodgkin's B lymphomas via NF-kappaB-dependent induction of HIF-1alpha. *Leukemia* 29: 1163-1176.
33. Morrison, S. J., D. E. Wright, and I. L. Weissman. 1997. Cyclophosphamide/granulocyte colony-stimulating factor induces hematopoietic stem cells to proliferate prior to mobilization. *Proc Natl Acad Sci U S A* 94: 1908-1913.
34. Waterstrat, A., Y. Liang, C. F. Swiderski, B. J. Shelton, and G. Van Zant. 2010. Congenic interval of CD45/Ly-5 congenic mice contains multiple genes that may influence hematopoietic stem cell engraftment. *Blood* 115: 408-417.
35. Adams, J. M., A. W. Harris, C. A. Pinkert, L. M. Corcoran, W. S. Alexander, S. Cory, R. D. Palmiter, and R. L. Brinster. 1985. The c-myc oncogene driven by immunoglobulin enhancers induces lymphoid malignancy in transgenic mice. *Nature* 318: 533-538.
36. He, W., S. Holtkamp, S. M. Hergenhan, K. Kraus, A. de Juan, J. Weber, P. Bradfield, J. M. P. Grenier, J. Pelletier, D. Druzd, C. S. Chen, L. M. Ince, S. Bierschenk, R. Pick, M. Sperandio, M. Aurrand-Lions, and C. Scheiermann. 2018. Circadian Expression of Migratory Factors Establishes Lineage-Specific Signatures that Guide the Homing of Leukocyte Subsets to Tissues. *Immunity* 49: 1175-1190 e1177.
37. Zhang, X., and Y. Wang. 2018. GRASP55 facilitates autophagosome maturation under glucose deprivation. *Mol Cell Oncol* 5: e1494948.
38. Maclean, K. H., F. C. Dorsey, J. L. Cleveland, and M. B. Kastan. 2008. Targeting lysosomal degradation induces p53-dependent cell death and prevents cancer in mouse models of lymphomagenesis. *J Clin Invest* 118: 79-88.
39. Imhof, B. A., C. Zimmerli, G. Gliki, D. Ducrest-Gay, P. Juillard, P. Hammel, R. Adams, and M. Aurrand-Lions. 2007. Pulmonary dysfunction and impaired granulocyte homeostasis result in poor survival of Jam-C-deficient mice. *J Pathol* 212: 198-208.
40. Zhang, X., and Y. Wang. 2016. Glycosylation Quality Control by the Golgi Structure. *J Mol Biol* 428: 3183-3193.
41. Rabouille, C., and A. D. Linstedt. 2016. GRASP: A Multitasking Tether. *Front Cell Dev Biol* 4: 1.
42. Nishida, C., K. Kusubata, Y. Tashiro, I. Gritli, A. Sato, M. Ohki-Koizumi, Y. Morita, M. Nagano, T. Sakamoto, N. Koshikawa, T. Kuchimaru, S. Kizaka-Kondoh, M. Seiki, H. Nakauchi, B. Heissig, and K. Hattori. 2012. MT1-MMP plays a critical role in hematopoiesis by regulating HIF-mediated chemokine/cytokine gene transcription within niche cells. *Blood* 119: 5405-5416.

43. Baramova, E. N., K. Bajou, A. Remacle, C. L'Hoir, H. W. Krell, U. H. Weidle, A. Noel, and J. M. Foidart. 1997. Involvement of PA/plasmin system in the processing of pro-MMP-9 and in the second step of pro-MMP-2 activation. *FEBS Lett* 405: 157-162.
44. Pietras, E. M., C. Mirantes-Barbeito, S. Fong, D. Loeffler, L. V. Kovtonyuk, S. Zhang, R. Lakshminarasimhan, C. P. Chin, J. M. Techner, B. Will, C. Nerlov, U. Steidl, M. G. Manz, T. Schroeder, and E. Passegue. 2016. Chronic interleukin-1 exposure drives haematopoietic stem cells towards precocious myeloid differentiation at the expense of self-renewal. *Nat Cell Biol* 18: 607-618.
45. Duran, J. M., C. Anjard, C. Stefan, W. F. Loomis, and V. Malhotra. 2010. Unconventional secretion of Acb1 is mediated by autophagosomes. *J Cell Biol* 188: 527-536.
46. Ivarsson, Y. 2012. Plasticity of PDZ domains in ligand recognition and signaling. *FEBS Lett* 586: 2638-2647.
47. Zhang, X., and Y. Wang. 2018. The Golgi stacking protein GORASP2/GRASP55 serves as an energy sensor to promote autophagosome maturation under glucose starvation. *Autophagy* 14: 1649-1651.
48. Meynet, O., B. Zunino, L. Happo, L. A. Pradelli, J. Chiche, M. A. Jacquin, L. Mondragon, J. F. Tanti, B. Taillan, G. Garnier, J. Reverso-Meinietti, N. Mounier, J. F. Michiels, E. M. Michalak, M. Carles, C. L. Scott, and J. E. Ricci. 2013. Caloric restriction modulates Mcl-1 expression and sensitizes lymphomas to BH3 mimetic in mice. *Blood* 122: 2402-2411.

Legend to Figures

Figure 1: Regulated expression of GRASP55 during early mouse hematopoietic cell differentiation. (A) Flow-cytometry gating strategy used to define hematopoietic stem and progenitor cells (HSPC). Representative dot-plot for wild-type mouse is shown. Hematopoietic Stem Cells and Multi-Potent Progenitor 1 (HSC-MPP1) are defined as LSK (Lin^- $Sca\text{-}1^+$ $c\text{-}Kit^+$) $CD150^+$ $CD48^-$, Multi-Potent Progenitor 2 MPP2 as LSK $CD150^+$ $CD48^+$, MMP3-4 as LSK $CD150^-$ $CD48^+$. Common Myeloid Progenitors (CMP) and Granulocyte Macrophage Progenitor (GMP) are respectively defined as LK (Lin^- $Sca\text{-}1^-$ $c\text{-}Kit^+$) $CD127^-CD16/32^-$ and LK $CD127^-CD16/32^+$. **(B)** Heat-map representation of relative mRNA expression as detected by RT-qPCR on 500 sorted cells. Actin expression levels were used for normalization. **(C)** Histogram showing changes in GRASP55 expression as measured by flow-cytometry. Results are expressed as fold changes relative to mean fluorescence intensity signals obtained for HSC-MPP1 subset. n=4 mice, * $p< 0.05$, ** $p< 0.01$. **(D)** Representative western-blot against GRASP55 on cell lysates obtained from 20 000 sorted cells. Ponceau red staining is shown as loading control. **(E)** Representative pictures of GRASP55 immunostaining on indicated cells isolated by flow-cytometry cell sorting. Cells isolated from *Grasp55*$^{-/-}$ mice were used as control. n= 3 mice. **(F)** Summed pixel intensities of individual objects found in individual confocal planes of Z stacks acquired on five HSC-MPP1, eight MPP2 and six MPP3-4 cells. *** $p < 0.001$. **(G)** Three dimensional quantification expressed as the volume of the largest vesiculo-tubular structures found in HSC-MPP1, MPP2 and MPP3-4 cells analyzed in (E). A significant enlargement of GRASP55 stained structures was found in MPP3-4. * $p < 0.05$, ** $p< 0.01$.

Figure 2: Early hematopoietic differentiation in *Grasp55*$^{-/-}$ mice. (A) Absolute numbers of bone marrow cells isolated from *Grasp55*$^{-/-}$ and control littermate mice. Results are expressed

as mean +/- SEM of cell numbers isolated from two legs per mice (n=6 per group). **(B-D)** Relative frequencies of LSK ($Lin^{Neg}Sca^{Pos}Kit^{Pos}$) cells (B), HSC-MPP1, MPP2 and MPP3-4 cells (C) and CMP and GMP (D) found in the bone marrow of *Grasp55*$^{-/-}$ and control littermate mice. Flow-cytometry gating strategy used to define HSPC in control and Grasp-55 deficient mouse is described in Fig. 1A. **(E)** Graph showing the relative Median Fluorescence Intensity (MFI) detected by flow cytometry for JAM-C staining on HSC-MMP1, MPP2, MPP3-4 cells isolated from *Grasp55*$^{-/-}$ and control littermate mice. Results are expressed as mean +/- SEM. Data are representative of six independent experiments.

Figure 3 : HSC mobilization is not affected by *Grasp55* deficiency.

(A) Relative frequencies of LSK ($Lin^{Neg}Sca^{Pos}Kit^{Pos}$) cells found in the bone marrow of *Grasp55*$^{-/-}$ and control littermate mice after HSC mobilization by CY/G-CSF. NaCl treated mice are used as control. **(B)** Relative frequencies of LSK cells found in blood of CY/G-CSF or NaCl injected *Grasp55*$^{-/-}$ and Grasp+/+ mice. **(C)** Number of CFU-C mobilized into blood from *Grasp55*$^{-/-}$ and control littermate mice after CY/G-CSF. Each symbol represents the average of colony numbers obtained per mice (2.10^5 cells/well, two wells per mice). * p< 0.05, ** p< 0.01, *** p< 0.001. Results from a single experiment with n= 3 to 4 mice are shown.

Figure 4 : Competitive engraftment of *Grasp55* deficient bone marrow cells.

(A) Experimental design of competitive bone marrow transplantation. The same number of *Grasp55*$^{+/+}$ or *Grasp55*$^{-/-}$ donor (CD45.2) cells were mixed in 1:1 ratio with competitor (CD45.1/2) bone marrow cells (See Sup Fig. 4A) and injected into CD45.1 lethally irradiated recipients. **(B)** Graph showing the frequency of CD45.2 donor cells in the blood of recipient mice engrafted either with *Grasp55*$^{+/+}$ (white dots) or *Grasp55*$^{-/-}$ (filled black dots) donor

762 cells. *p< 0.05 **(C-F)** Donor specific $CD4^+$ T cells (C), $CD8^+$ T cells (D), $B220^+$ B cells (E)
763 and $CD11b^+$ myeloid cells (F) frequencies in the blood of mice transplanted with *Grasp55*$^{+/+}$
764 (white dots) or *Grasp55*$^{-/-}$ (filled black dots) bone marrow. **(G-H)** Relative frequencies of
765 donor and competitor LSK ($Lin^{Neg}Sca^{Pos}Kit^{Pos}$), HSC-MPP1, MPP2, MPP3-4 (G), CMP and
766 GMP (H) cells found in the bone marrow of mixed chimera engrafted with *Grasp55*$^{+/+}$ or
767 *Grasp55*$^{-/-}$ donor cells 18 weeks after cell injection. Results are expressed as mean +/- SEM.
768 Data show results of one representative experiment from two independent experiments.
769
770
771 **Figure 5 : *Grasp55* silencing inhibits Eμ-myc leukemic engraftment**
772 **(A)** Phenotype of primary Eμ-myc clone assessed by flow cytometry and showing the pre-B
773 cell nature of leukemic cells. **(B)** JAM-B expression by the primary Eμ-myc clone shown in
774 (A). **(C)** Western-blot analysis of Eμ-myc cells one week after transfection with Ctl-GFP or
775 shGRASP-55 lentivirus using GRASPP55 (upper panel) or actin (lower panel) antibodies. **(D)**
776 Proliferation of Eμ-Myc $GRASP55^{WT}$ and Eμ-Myc $GRASP55^{KD}$ in complete medium was
777 determined using ATPmetry (Cell Titer Glow, Promega). Results are expressed as mean
778 RLU values +/- SEM obtained from four replicates. Doubling times are 16.20+/-1.468 hours
779 for Eμ-Myc $GRASP55^{WT}$ and 20.10+/-3.869 hours for Eμ-Myc $GRASP55^{KD}$. **(E-G)** Tumor
780 invasion of Eμ-myc cells in the indicated organ nine days after injection of 50.000
781 $GRASP55^{WT}$ or $GRASP55^{KD}$ Eμ-myc cells in CD45.1 mice. Tumor invasion in spleen is
782 revealed by spleen weight and percentage of $CD45.2^+GFP^+$ cells (E). Percentages of $CD45.2^+$
783 GFP^+ cells in bone (F) and blood (G) are shown. Results are expressed as mean +/- SEM. n =
784 6 mice per group. One representative experiment from two independent experiments is
785 shown. ** p<0.01.
786

Figure 6 : *Grasp55* silencing decreases leukemic cell survival

(A) Left panel: dot plot showing the indicated fluorescence of the mix of $GRASP55^{WT}$ ($GFP^{+}Calcein\ violet^{-}$) and $GRASP55^{KD}$ ($GFP^{+}Calcein\ violet^{+}$) Eμ-myc cells before injection. Right panels: dot plots showing the GFP and Calcein violet fluorescence signals 16 hours after injection in the indicated organs. Relative proportions of $GRASP55^{WT}$ ($Calcein\ violet^{-}$) and $GRASP55^{KD}$ (Calcein violet+) cells within the GFP+ compartments are indicated. **(B)** Absolute number of $GRASP55^{WT}$ and $GRASP55^{KD}$ Eμ-myc cells in the indicated organs sixteen hours after injection. Each symbol represents an individual mouse. n = 6 mice per group. Results obtained in a single experiment are expressed as mean +/- SD. *** $p<0.001$.

Figure 7: Grasp55 silencing increases apoptosis

(A) Histograms showing Caspase 3/7 activity of $GRASP55^{WT}$ (white bar) and $GRASP55^{KD}$ Eμ-myc cells (black bar) twelve hours after plating and expressed as fold increase over time 0. **(B)** Dot plots showing representative results of AnnexinV and iodinium propide (PI) or cytometry staining of $GRASP55^{WT}$ and $GRASP55^{KD}$ Eμ-myc cells twelve hours after plating in fresh medium. **(C)** Quantification of results shown in (B) showing significant decrease survival of $GRASP55^{KD}$ as compared to $GRASP55^{WT}$ Eμ-myc cells twelve hours after plating. Conversely, significant increases in early and late apoptosis are observed * $p<0.05$, *** $p<0.001$. **(D)** Graph showing Eμ-myc cell survival upon glucose starvation after 96 hours. Results are expressed as percentage of survival obtained in complete medium. * $p<0.05$. One representative experiment from three independent experiments is shown.

Figure 8: GRASP55 is not required for autophagy. (A) Cytotoxicity of chloroquine on $GRASP55^{WT}$ and $GRASP55^{KO}$ EμMyc and $Grasp55^{+/+}$ and $Grasp55^{-/-}$ MEFs at 24 hours using Cell Titer Glo assay. **(B)** IC50 of chloroquine on $GRASP55^{WT}$ and $GRASP55^{KO}$ EμMyc and

812 Grasp55$^{+/+}$ and Grasp55$^{-/-}$ MEFs at 24hours. Results of one representative experiment from
813 three independent experiments are shown. **(C-D)** Western blot against GRASP55 and LC3 on
814 GRASP55^{WT} and GRASP55^{KO} EμMyc (C) and Grasp55$^{+/+}$ and Grasp55$^{-/-}$ MEFs (D) after 24
815 hours chloroquine treatment. Tubulin was used as loading control. One representative
816 experiment from three independent experiments is shown.
817

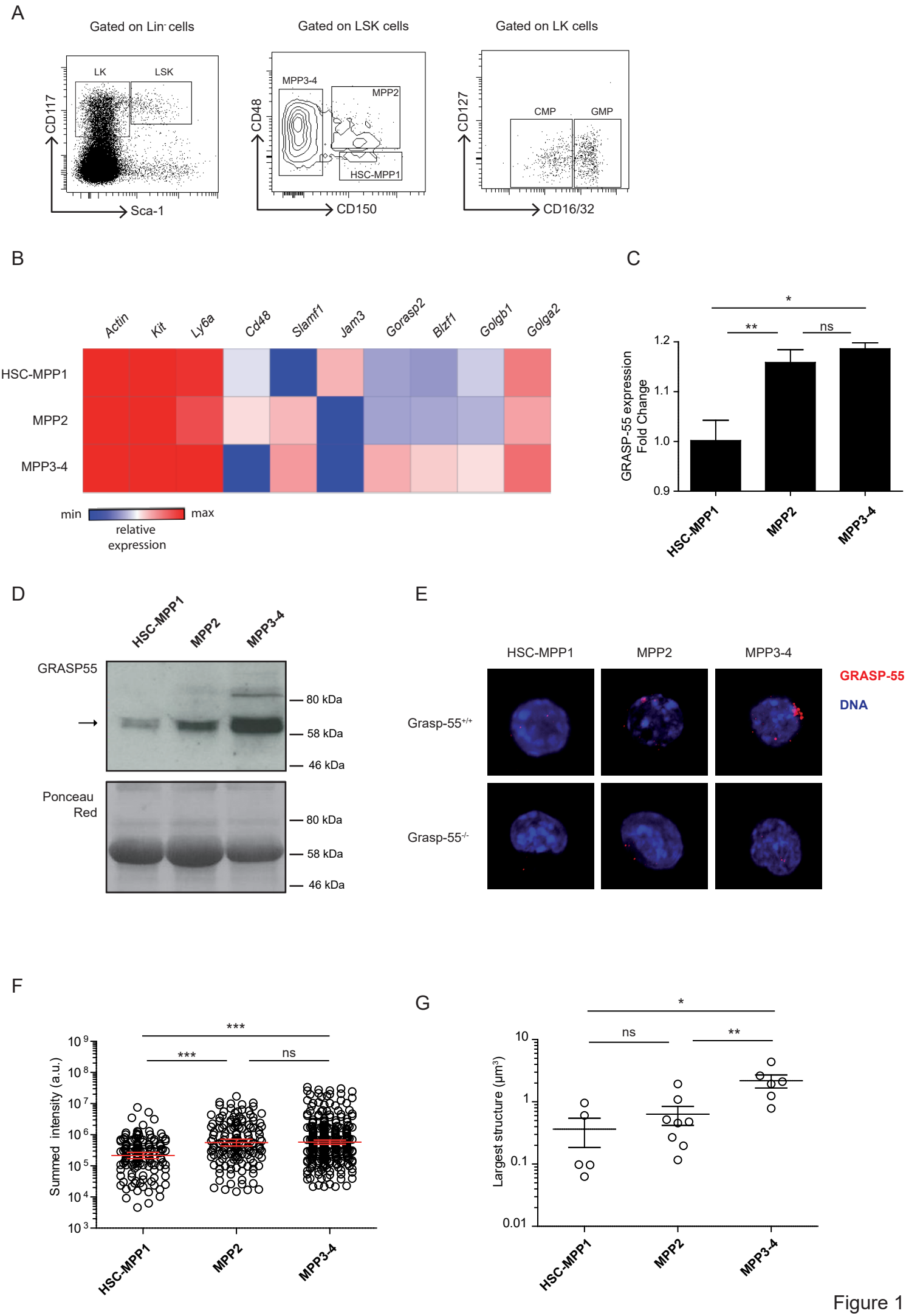
A
Gated on Lin- cells
Gated on LSK cells
Gated on LK cells
LK
LSK
CD117
Sca-1
MPP3-4
MPP2
HSC-MPP1
CD48
CD150
CMP
GMP
CD127
CD16/32
B
Actin
Kit
Ly6a
Cd48
Slamf1
Jam3
Gorasp2
Blzf1
Golgb1
Golga2
HSC-MPP1
MPP2
MPP3-4
min
max
relative expression
C
GRASP-55 expression Fold Change
1.2
1.1
1.0
0.9
*
**
ns
HSC-MPP1
MPP2
MPP3-4
D
HSC-MPP1
MPP2
MPP3-4
GRASP55
80 kDa
58 kDa
46 kDa
Ponceau Red
80 kDa
58 kDa
46 kDa
E
HSC-MPP1
MPP2
MPP3-4
GRASP-55
DNA
Grasp-55+/+
Grasp-55-/-
F
Summed intensity (a.u.)
10 9
10 8
10 7
10 6
10 5
10 4
10 3
***
***
ns
HSC-MPP1
MPP2
MPP3-4
G
Largest structure (µm3)
10
1
0.1
0.01
*
ns
**
HSC-MPP1
MPP2
MPP3-4

Figure 1

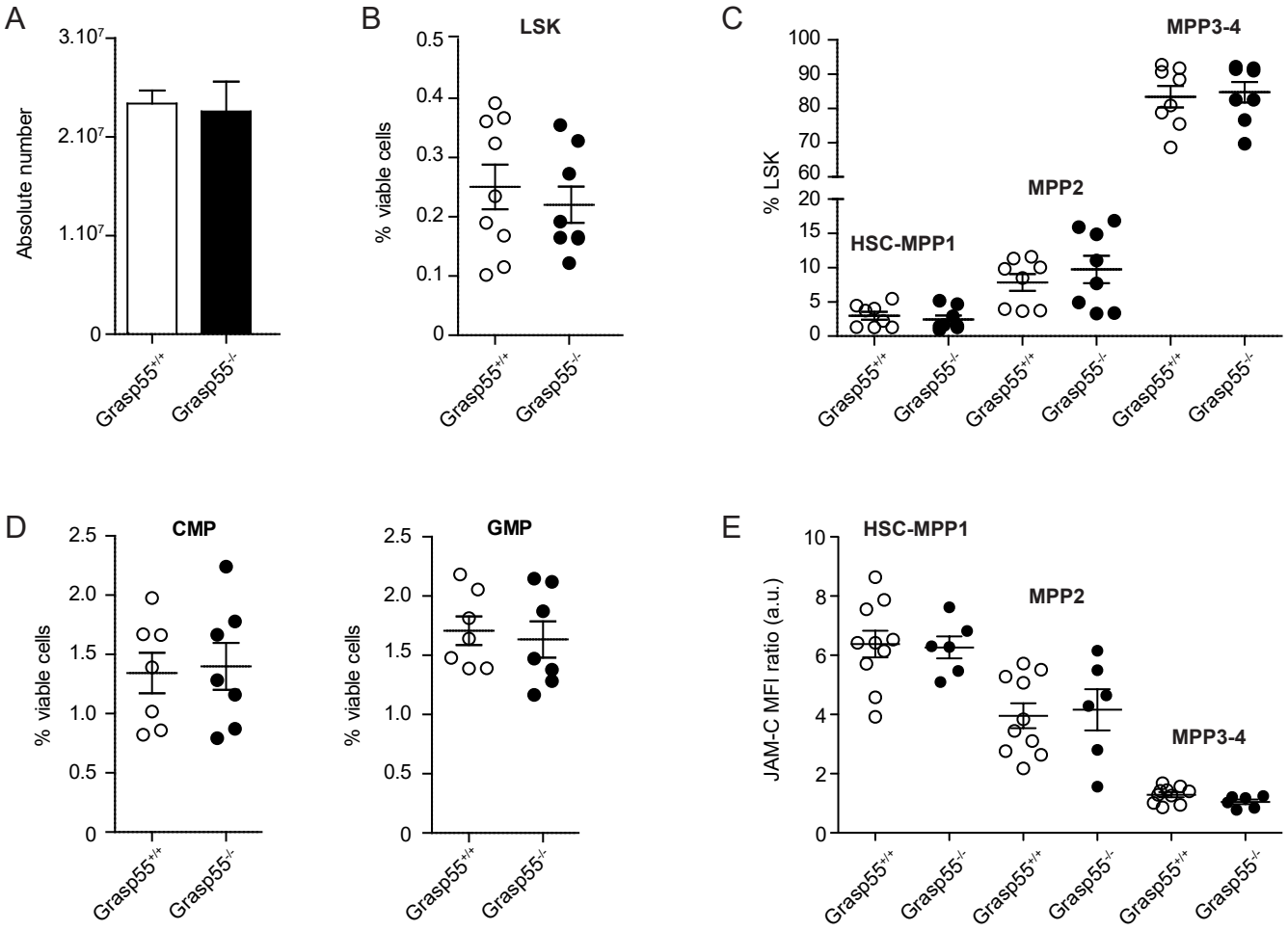
A
Absolute number
3.10⁷
2.10⁷
1.10⁷
0
Grasp55+/+
Grasp55-/-
B
LSK
% viable cells
0.5
0.4
0.3
0.2
0.1
0
C
% LSK
HSC-MPP1
MPP2
MPP3-4
100
90
80
70
60
20
15
10
5
0
D
CMP
GMP
% viable cells
2.5
2.0
1.5
1.0
0.5
0
E
JAM-C MFI ratio (a.u.)
HSC-MPP1
MPP2
MPP3-4
10
8
6
4
2
0

Figure 2

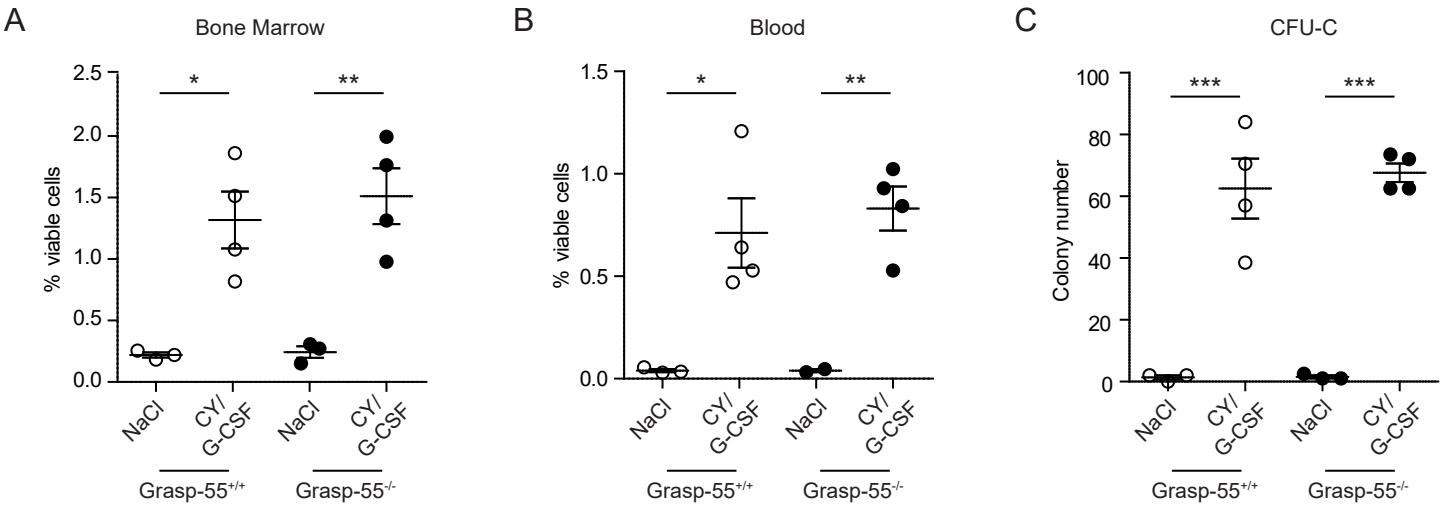
A
Bone Marrow
% viable cells
2.5
2.0
1.5
1.0
0.5
0.0
*
**
NaCl
CY/ G-CSF
NaCl
CY/ G-CSF
Grasp-55+/+
Grasp-55-/-
B
Blood
% viable cells
1.5
1.0
0.5
0.0
*
**
NaCl
CY/ G-CSF
NaCl
CY/ G-CSF
Grasp-55+/+
Grasp-55-/-
C
CFU-C
Colony number
100
80
60
40
20
0
***
***
NaCl
CY/ G-CSF
NaCl
CY/ G-CSF
Grasp-55+/+
Grasp-55-/-

Figure 3

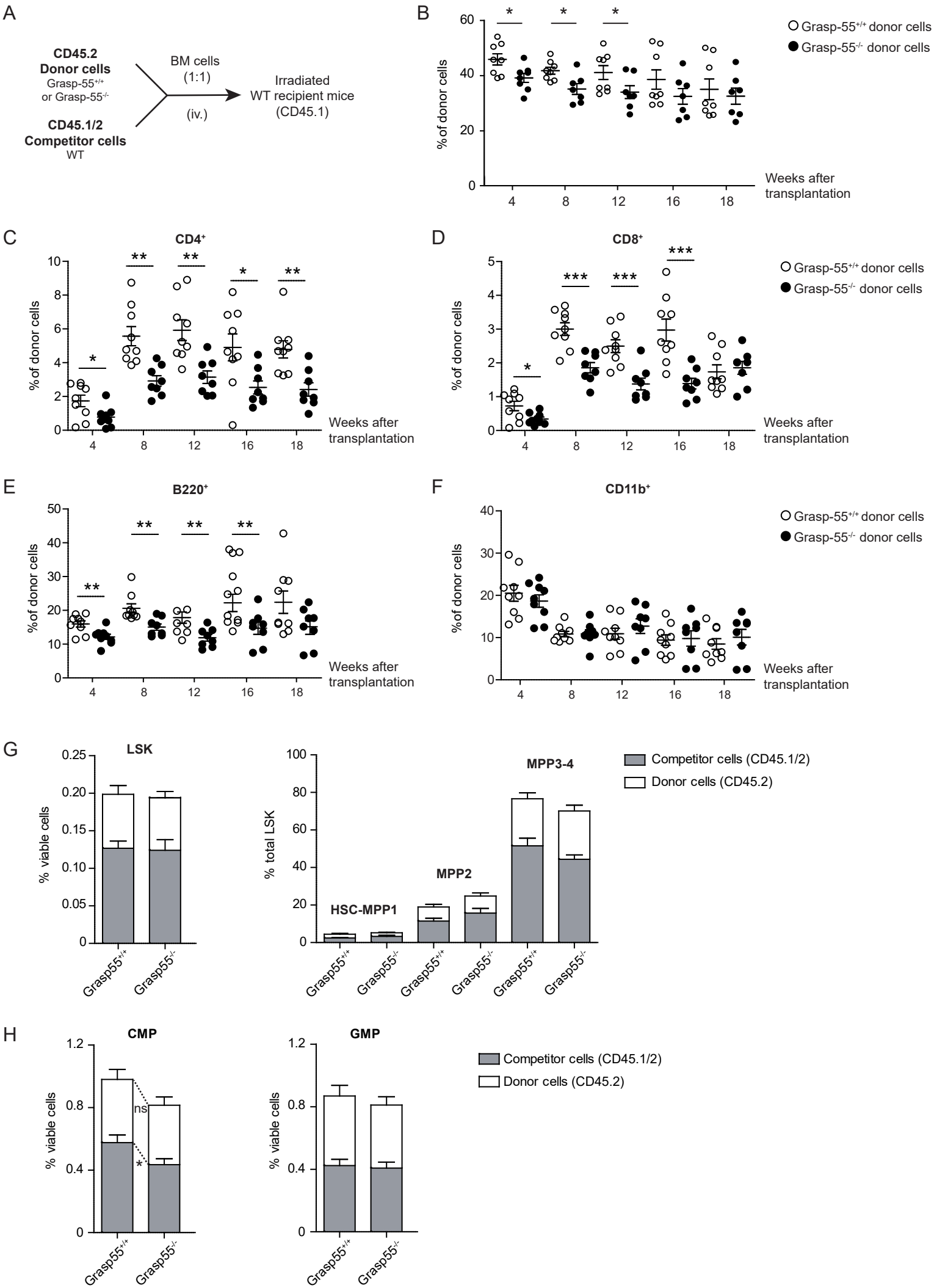
A
CD45.2
Donor cells
Grasp-55+/+
or Grasp-55-/-
CD45.1/2
Competitor cells
WT
BM cells
(1:1)
(iv.)
Irradiated
WT recipient mice
(CD45.1)
B
Grasp-55+/+ donor cells
Grasp-55-/- donor cells
% of donor cells
Weeks after
transplantation
C
CD4+
D
CD8+
E
B220+
F
CD11b+
G
LSK
% viable cells
% total LSK
MPP3-4
MPP2
HSC-MPP1
Competitor cells (CD45.1/2)
Donor cells (CD45.2)
Grasp55+/+
Grasp55-/-
H
CMP
GMP
ns

Figure 4

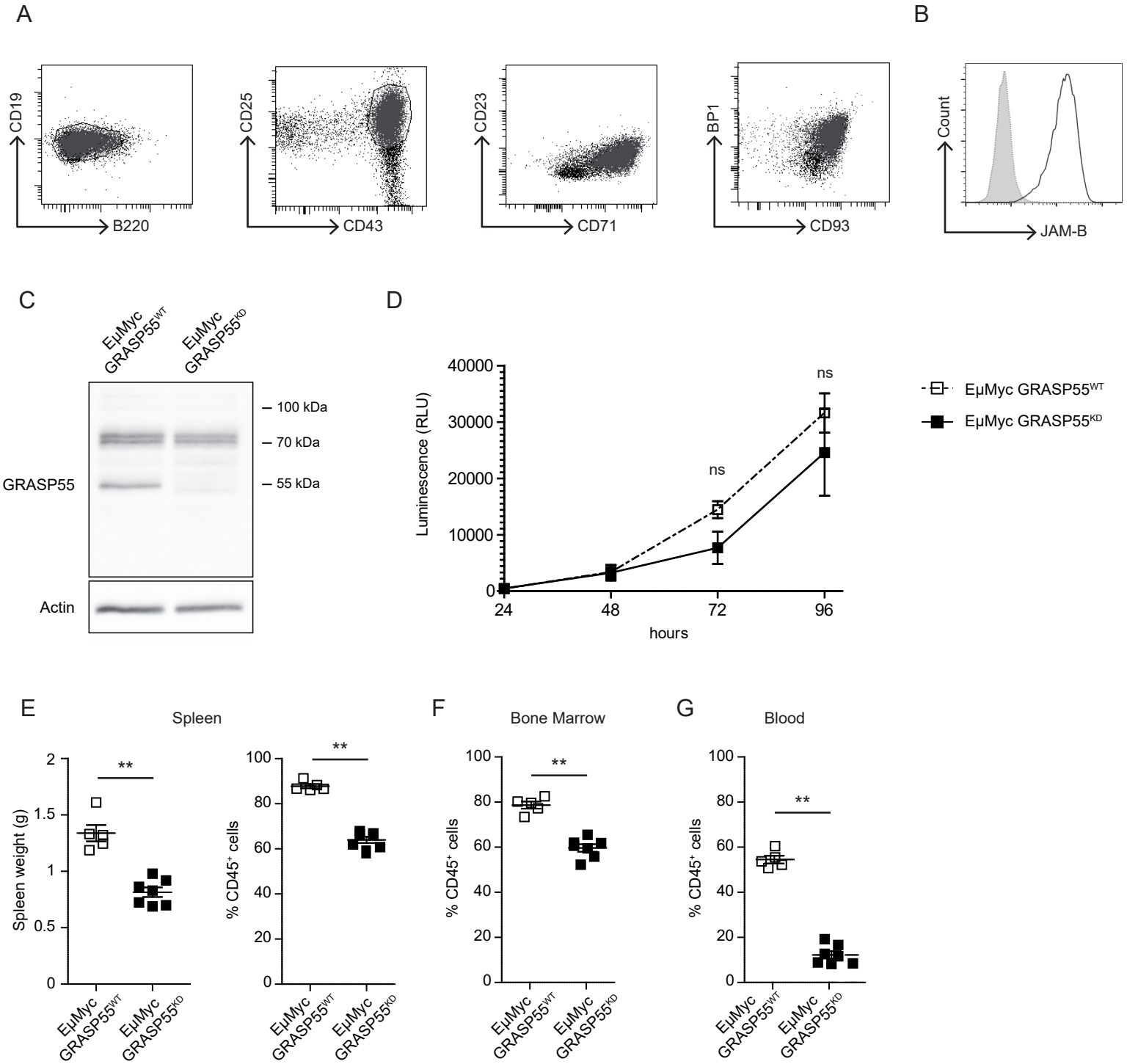
A
CD19
B220
CD25
CD43
CD23
CD71
BP1
CD93
B
Count
JAM-B
C
EμMyc GRASP55WT
EμMyc GRASP55KD
100 kDa
70 kDa
55 kDa
GRASP55
Actin
D
Luminescence (RLU)
40000
30000
20000
10000
0
ns
ns
24
48
72
96
hours
EμMyc GRASP55WT
EμMyc GRASP55KD
E
Spleen
Spleen weight (g)
2
1.5
1
0.5
0
**
% CD45+ cells
100
80
60
40
20
0
**
F
Bone Marrow
% CD45+ cells
**
G
Blood
% CD45+ cells
**

Figure 5

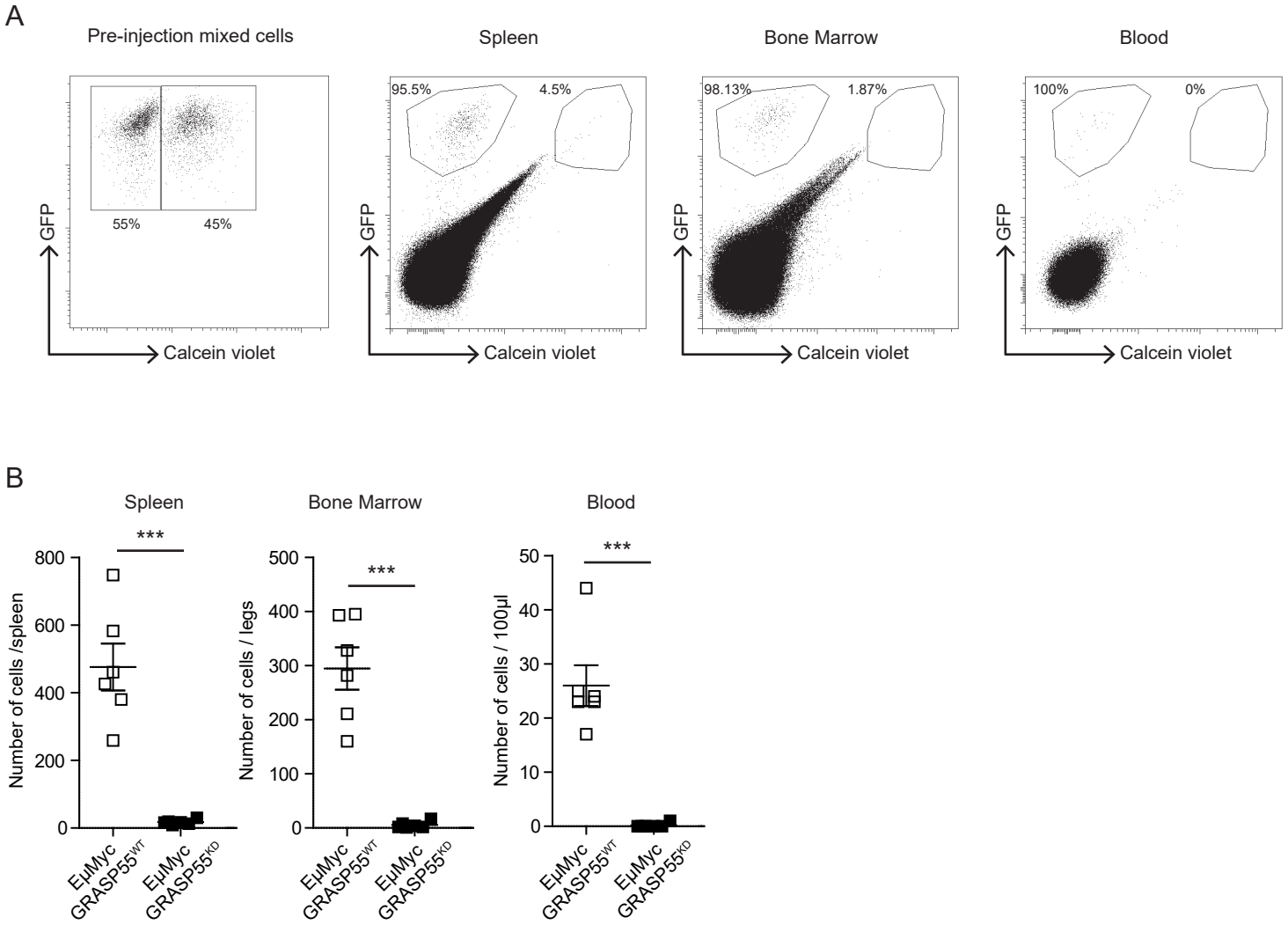
A
Pre-injection mixed cells
Spleen
Bone Marrow
Blood
GFP
Calcein violet
55%
45%
95.5%
4.5%
98.13%
1.87%
100%
0%
B
Spleen
Bone Marrow
Blood
***
Number of cells /spleen
Number of cells / legs
Number of cells / 100µl
EµMyc GRASP55WT
EµMyc GRASP55KD

Figure 6

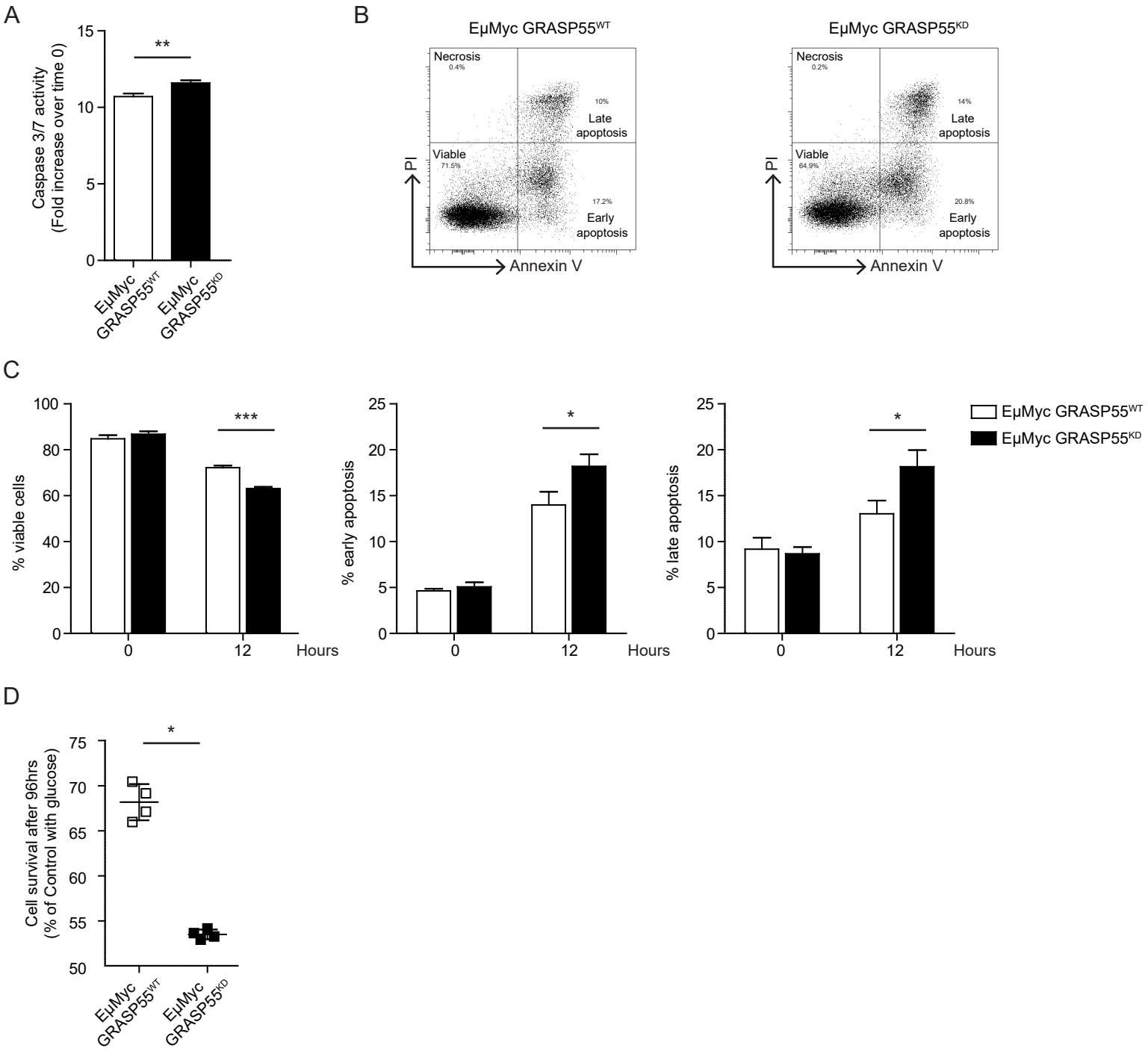
A
Caspase 3/7 activity
(Fold increase over time 0)
15
10
5
0
**
EμMyc GRASP55WT
EμMyc GRASP55KD
B
EμMyc GRASP55WT
EμMyc GRASP55KD
Necrosis
0.4%
10%
Late apoptosis
Viable
71.5%
17.2%
Early apoptosis
PI
Annexin V
Necrosis
0.2%
14%
Late apoptosis
Viable
64.9%
20.8%
Early apoptosis
PI
Annexin V
C
% viable cells
100
80
60
40
20
0
***
0
12
Hours
% early apoptosis
25
20
15
10
5
0
*
0
12
Hours
% late apoptosis
25
20
15
10
5
0
*
0
12
Hours
EμMyc GRASP55WT
EμMyc GRASP55KD
D
Cell survival after 96hrs
(% of Control with glucose)
75
70
65
60
55
50
*
EμMyc GRASP55WT
EμMyc GRASP55KD

Figure 7

A

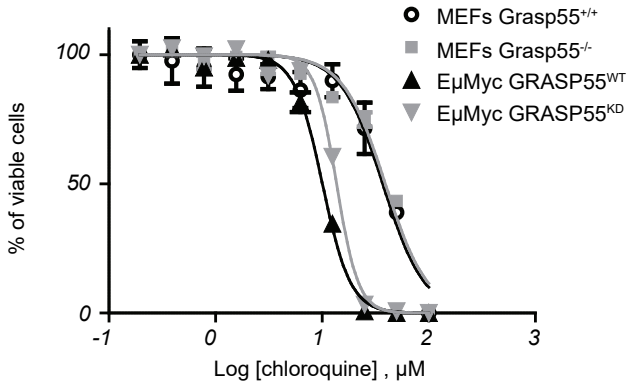

B

	IC50 (μM)
EμMyc GRASP55^{WT}	8.85
EμMyc GRASP55^{KD}	11.56
MEFs Grasp-55$^{+/+}$	37.01
MEFs Grasp-55$^{-/-}$	37.53

C

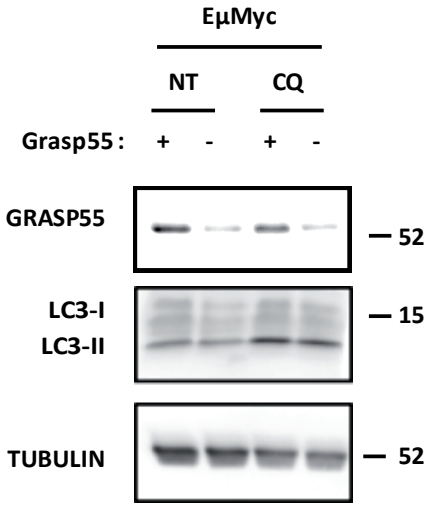

D

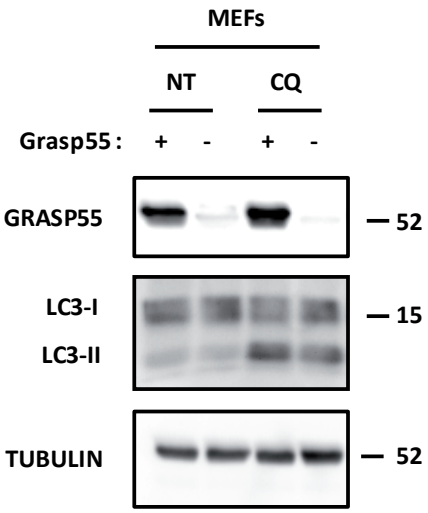

Figure 8

GRASP55 is dispensable for normal hematopoiesis but necessary for Myc-dependent leukemic growth.

Anne-Laure Bailly[*], Julien M.P. Grenier[*], Amandine Cartier-Michaud[*], Florence Bardin[*], Marielle Balzano[*], Armelle Goubard[*], Jean-Claude Lissitzky[*], Maria De Grandis†, Stéphane J.C. Mancini[*], Arnauld Sergé[*] and Michel Aurrand-Lions[*#]

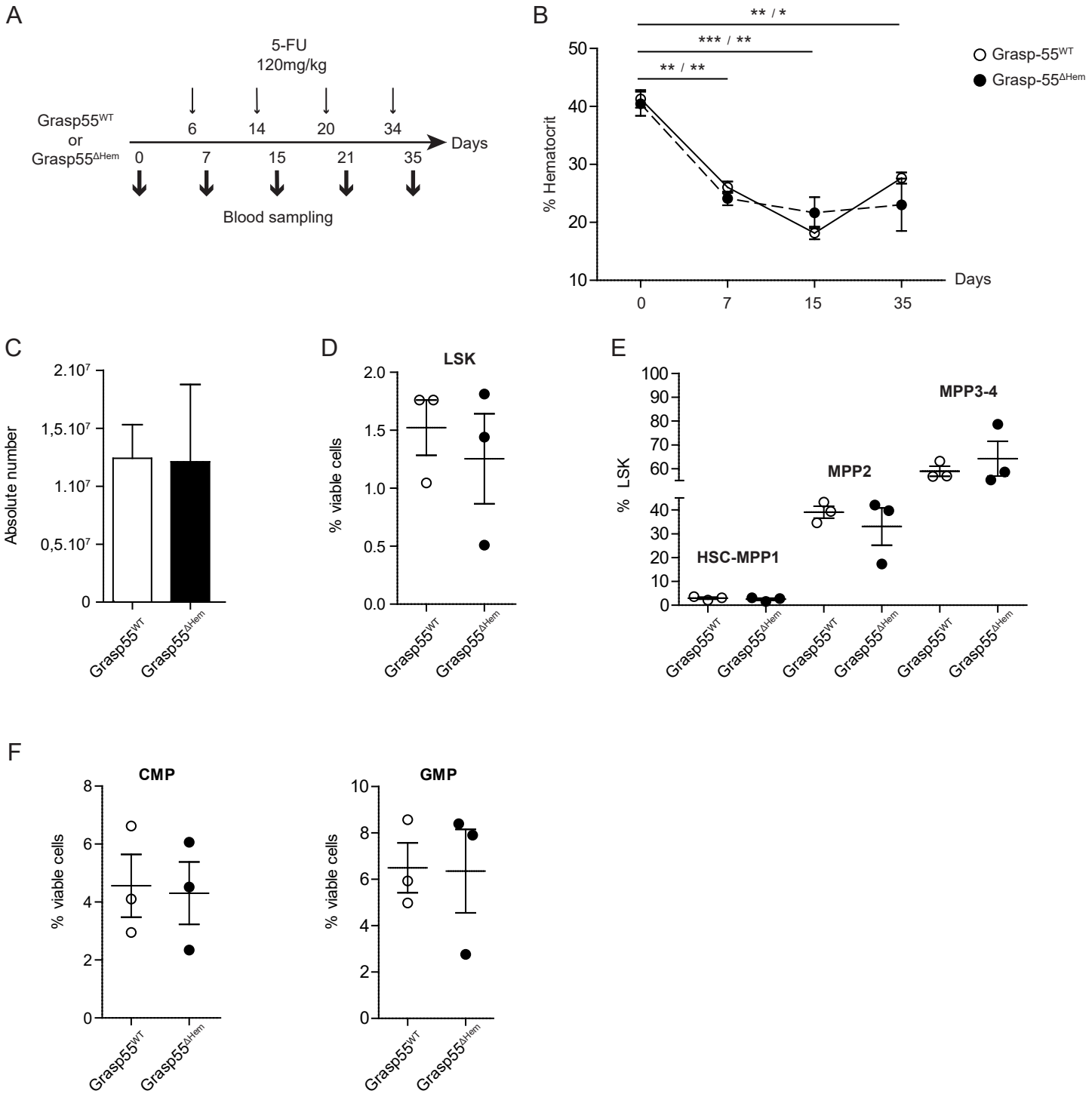

Supplementary Figure 1: Hematopoietic stress response of *Grasp55*$^{-/-}$ mice. (A) Experimental design for HSC exhaustion after 5-fluoro-uracil (5-FU) treatment: *Grasp55*$^{fl/-}$ Vav-cre^{Neg} and *Grasp55*$^{fl/-}$Vav-cre^{Pos} mice were injected weekly with 120mg/kg 5-FU and bled one day later over five weeks. Mice were sacrificed at D35 after first injection. **(B)** Hematocrit levels of Grasp55$^{fl/-}$Vav-cre^{Neg} and Grasp55$^{fl/-}$Vav-cre^{Pos} mice at indicated time points. (n=3 per group). * p< 0.05, ** p< 0.01, *** p<0.0001. **(C)** Absolute numbers of bone marrow cells isolated from *Grasp55*$^{fl/-}$Vav-cre^{Neg} and *Grasp55*$^{fl/-}$Vav-cre^{Pos} animals at sacrifice. **(D-F)** Relative frequencies of LSK (D), HSC-MPP1, MPP2, MPP3-4 (E), CMP and GMP (F) found in the bone marrow of from *Grasp55*$^{fl/-}$Vav-cre^{Neg} and *Grasp55*$^{fl/-}$Vav-cre^{Pos} animals after five injections of 5-FU. Results from a single experiment are shown.

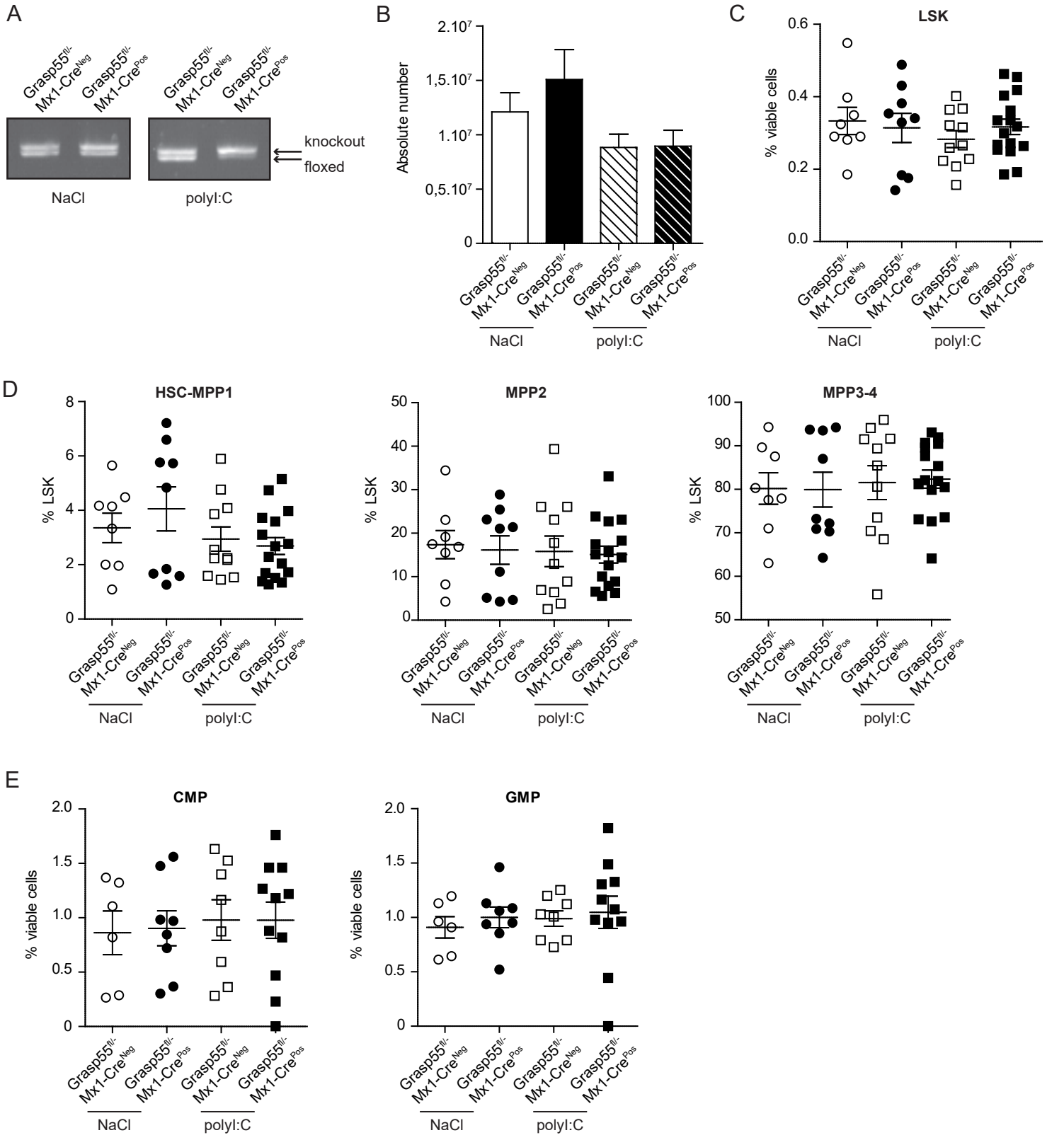

Supplementary Figure 2: Induced deletion of Grasp55 in adult hematopoietic cells does not result in impaired hematopoiesis. **(A)** Agarose gel of the PCR-amplified products obtained from white blood cells isolated from Grasp55fl/- Mx1-CreNeg and Grasp55fl/- Mx1-CrePos fifteen days after injection with polyI:C or NaCl. **(B-E)** Absolute numbers of bone marrow cells (B) and relative frequencies of LSK (C) HSC-MPP1, MPP2, MPP3-4 (D) CMP and GMP (E) found in the bone marrow of from Grasp55fl/- Mx1-CreNeg and Grasp55fl/- Mx1-CrePos one month after Mx1-cre induction with polyI:C. NaCl injected animals and mice lacking Mx1-Cre expression are used as control. No significant difference between experimental groups is observed. Results represent the pool of two independent experiments with n=3 to 5 mice per group.

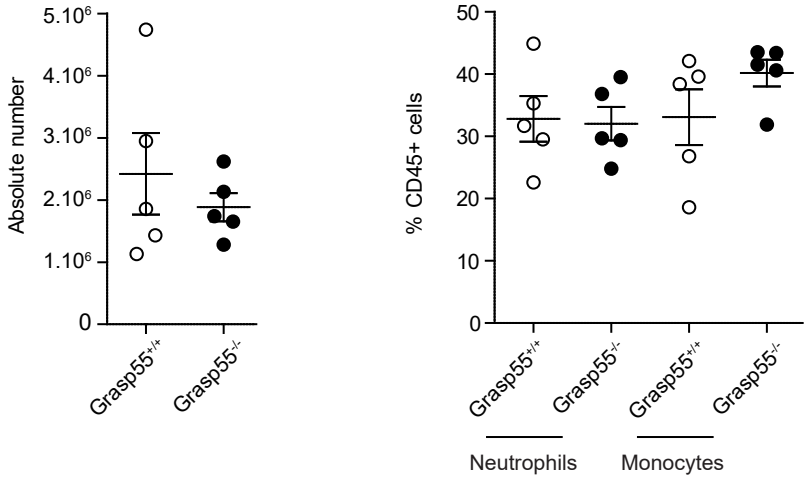

Supplementary Figure 3: GRASP-55 is dispensable for inflammatory cells recruitment in thioglycollate-induced peritonitis. Absolute number of total cells (left panel) and leukocytes frequencies (right panel) in peritoneal lavage fluids of Grasp55$^{-/-}$ and Grasp55$^{+/+}$ chimeric mice 18 hours after thioglycollate i.p. injection. One representative experiment is shown (from three independent experiments).

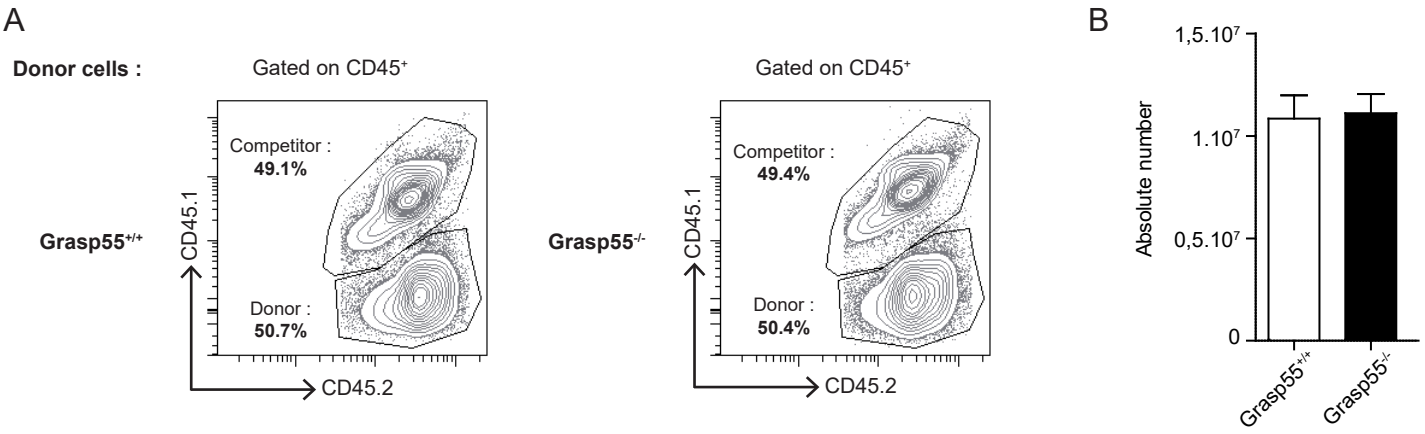

Supplementary Figure 4: Competitive bone marrow transplantation

(A) Representative dot plots showing the 1:1 ratio of donor and competitor cells for the indicated experimental group used in Figure 4 (Grasp55-/-, left panel and Grasp55+/+, right panel). **(B)** Absolute number of bone marrow cells in recipient mice 18 weeks after engraftment with *Grasp55*$^{+/+}$ and *Grasp55*$^{-/-}$ donor cells.